NUMERICAL STUDY OF ENTROPY GENERATION EFFECT IN Al_2O_3 / METHANOL NANOFLUID FLOW OVER A SWIRLING DISK

By

MEHWISH RAZEEQ

NATIONAL UNIVERSITY OF MODERN LANGUAGES

ISLAMABAD

2nd December, 2024

Numerical Study of Entropy Generation Effect in Al_2O_3 / Methanol Nanofluid Flow over a Swirling Disk

By

Mehwish Razeeq

MS Mathematics, National University of Modern Languages, Islamabad, 2024

A THESIS SUBMITTED IN PARTIAL FULFILMENT OF

THE REQUIREMENTS FOR THE DEGREE OF

MASTER OF SCIENCE

In **Mathematics**

To

FACULTY OF ENGINEERING & COMPUTING

NATIONAL UNIVERSITY OF MODERN LANGUAGES ISLAMABAD

THESIS AND DEFENSE APPROVAL FORM

The undersigned certify that they have read the following thesis, examined the defense, are satisfied with overall exam performance, and recommend the thesis to the Faculty of Engineering and Computing for acceptance.

Thesis Title: Numerical Study of Entropy Generation Effect in Al_2O_3 / Methanol Nanofluid Flow over a Swirling Disk

Submitted By: Mehwish Razeeq **Registration #:** 38 MS/MATH/F21

Master of Science in Mathematics (MS MATH)
Title of the Degree

Mathematics
Name of Discipline

Dr. ASIA ANJUM _____
Name of Research Supervisor Signature of Research Supervisor

DR. SADIA RIAZ _____
Name of HOD Signature of HOD

DR. NOMAN MALIK _____
Name of Dean (FEC) Signature of Dean (FEC)

2nd December, 2024

AUTHOR'S DECLARATION

I Mehwish Razeeq

Daughter of Muhammad Razeeq

Registration # 38 MS/MATH/F21

Discipline Mathematics

Candidate of **Master of Science in Mathematics (MS MATH)** at the National University of Modern Languages do hereby declare that the thesis **Numerical Study of Entropy Generation Effect in Al_2O_3 / Methanol Nanofluid Flow over a Swirling Disk** submitted by me in partial fulfillment of MS MATHS degree, is my original work, and has not been submitted or published earlier. I also solemnly declare that it shall not, in future, be submitted by me for obtaining any other degree from this or any other university or institution. I also understand that if evidence of plagiarism is found in my thesis/dissertation at any stage, even after the award of a degree, the work may be cancelled and the degree revoked.

_____
Signature of Candidate

Mehwish Razeeq
Name of Candidate

2nd December, 2024
Date

ABSTRACT

Title: Numerical Study of Entropy Generation Effect in Al_2O_3 / Methanol Nanofluid Flow over a Swirling Disk

This thesis presents a comprehensive numerical study for the effects of entropy generation on the flow of an Al_2O_3/Methanol nanofluid over a Swirling disk. The primary focus is to analyse the steady-state, incompressible flow characteristics and heat transfer dynamics of the nanofluid. The governing equations, which were originally expressed as partial differential equations (PDEs), are transformed into a set of nonlinear ordinary differential equations (ODEs) through similarity transformations. These transformed equations are then solved by using MATLAB's bvp-4c solver. The results are presented through graphs and tables, providing insights into the influence of these parameters on entropy generation and thermal conductivity. This study contributes to the understanding of nanofluid behaviors in rotating systems, offering potential applications in engineering and industrial processes.

TABLE OF CONTENTS

LIST OF TABLES

LIST OF FIGURES

LIST OF ABBREVIATIONS

BVP	Boundary value problem
IVP	Initial value problem
N_s	Entropy generation
ODEs	Ordinary differential equation
PDEs	Partial differential equation
Al_2O_3	Aluminium oxide
MATLAB	Matrix Laboratory
BVP4C	Boundary value problem for 4th-order colocation
Nu	Nusselt number
C_f	Skin Friction Coefficient
GE	Governing Equation

LIST OF SYMBOLS

μ	Fluid viscosity
ν	Kinematics viscosity
τ	Share stress
k	Thermal conductivity
α	Thermal diffusivity
c_p	Specific Heat
T_∞	Ambient temperature
ξ	Similarity variable
f	Dimensionless velocity
ϕ	Dimensionless concentration
Ec	Eckert number
Pr	Prandtl number
N_s	Entropy generation
Be	Bejan number
Br	Brinckmann number
k_f	Thermal conductivity of fluid
k_p	Thermal conductivity of nanoparticle
ρ_p	Density of nanoparticle
$(\rho c_p)_f$	Heat capacitance of fluid
$(\rho c_p)_p$	Heat capacitance of Nanoparticle
P	Pressure
N_{SH}	Entropy generation due to heat transfer
T_w	Temperature at wall
N_{SF}	Entropy generation due to viscous dissipation
u	Velocity component in the radial direction
v	Velocity component in tangential direction
V	Velocity vector
w	Velocity component in the axial direction
w_0	Uniform suction

z	Normal direction in cylindrical polar coordinates
F	Self-similar radial velocity
G	Self-similar tangential velocity
H	Self-similar axial velocity

ACKNOWLEDGMENT

First and foremost, I want to thank Almighty Allah, who made this study possible and successful. This study would not have been accomplished without the sincere support extended from several sources, for which I would like to express my heartfelt thankfulness and gratitude. I am profoundly grateful to my research supervisors, Dr. Asia Anjum, and my co-supervisor, Dr. Adnan Saeed, for their unwavering support and insightful guidance throughout my research journey. Their expertise, encouragement, and dedication were instrumental in shaping this thesis and ensuring its successful completion.

A special note of appreciation goes to my mother-in-law, Mrs. Zahida, for her unwavering support and for caring for my children, allowing me the time and peace of mind to focus on my research. Her help has been invaluable, and I am deeply thankful for her dedication and love. I am also profoundly grateful to my husband, Dr. Ahsan Raza, for his continuous guidance, support, and encouragement. His understanding and patience have been a pillar of strength throughout this journey.

Finally, I shall also acknowledge the extended assistance from the administration of the Department of Mathematics, who supported me throughout my research experience and simplified the challenges I faced. For all whom I did not mention, but I shall not neglect their significant contribution, thanks for everything.

DEDICATION

This is dedicated to my parents, who have loved me unconditionally and whose good example has taught me to work hard for the things I aspire to achieve.

CHAPTER 1

INTRODUCTION

1.1 Nanofluids

Nanofluids are specially designed fluids comprising two components: a base fluid (such as oil, water, or ethylene glycol) and small particles that are usually between one and one hundred nanometers in diameter. These nanoparticles can be derived from various materials, including metals (such as copper, silver, or gold), metal oxides (like alumina or titanium dioxide), carbon nanotubes, or other nanomaterials. In 1995, Choi *et al.* [1] introduced the creation of a novel type of heat transfer fluid by suspending small metal particles in conventional fluids. These "nanofluids" are anticipated to substantially enhance thermal conductivity, potentially reducing energy consumption in heat exchangers and various industrial applications. As discussed by Senthilraja *et al.* [2] nanofluids have numerous potential uses in industries such as automotive, microelectronics, nuclear, space, and power generation, where they serve to augment heat transmission and elevate energy efficiency.

In the automotive sector, Patel *et al*. [3] investigated nanofluids composed of minuscule particles, highlighting their capability to enhance system efficiency through effective heat transfer and reduced wear and tear. However, they noted that further research is needed to fully understand their benefits and address stability concerns. Ali *et al.* [4] investigated the behaviour of fluids containing micron-sized aluminium oxide particles, which studies the impact of magnetic fields, thermal radiation, and heat fluctuations. Their findings indicated that particle size and spacing significantly affect energy distribution and flow. Ahmad *et al*. [5] investigated the heat transfer characteristics and flow of a hybrid nanofluids, using silver and titanium dioxide in a water base. They simplified the governing equations to nonlinear differential equations and utilized Cattaneo-Christov's theory to account for the finite speed of heat transmission.

Similarly, Yasmin *et al*. [6] analyzed the impact of temperature and particle concentration on the properties of metal oxide nanofluids., with a particular emphasis on magnetic and electric fields, chemical stability, and oxidation resistance. These factors underscore the potential of metal oxide nanofluids in sustainable energy applications. Moreover, Fadhil *et al*. [7] investigated the use of nanofluids as a cost-effective solution for cooling electronic devices, heat exchangers, and chemical processes. They highlighted the enhanced heat-transfer qualities of liquids like water, oil, or ethylene glycol when used in nanofluid applications. Afzal *et al*. [8] described the role of entropy in analyzing blood-based hybrid nanofluids in rotating disks within industrial and medical settings through an optimal homotropy analysis approach.

Omid Mahian *et al*. [9] discussed the advantageous effects of nanofluids in enhancing the efficiency of solar collectors, water heaters, and thermal energy storage systems, emphasizing their role in addressing efficiency and environmental concerns. Moreover, Mahmod *et al*. [10] analyzed a mathematical model employing tri-hybrid nanofluids that demonstrated significant improvements in temperature profiles and rates, suggesting potential advancements in applications like metal coatings, aerospace, and medicine. Rafique *at al.* [11] discovered notable improvements in heat transfer in nanofluid thermal performance, which could have a wide range of industrial applications. Through the analysis of viscosity, joule heating, and other characteristics, Rafique *et al*. [12] investigated heat transfer in nanofluids containing carbon nanotubes and found that certain parameters lead to enhanced heat transfer rates. Also, Basit *et al*. [13] examined the use of hybrid nanofluids that integrate blood with nanoparticles. Compared to conventional nanofluids, these hybrid variants exhibit superior heat transfer properties, heralding new possibilities for their application in thermal management.

1.2 Entropy generation

Entropy is a fundamental concept in thermodynamics, physics, and information theory, representing the measure of a system's disorder or unpredictability. The term "entropy generation" refers to the quantity of entropy produced in a system through irreversible processes such as fluid flow, chemical reactions, and heat transfer. Understanding and controlling entropy generation is crucial for the development of ecologically sustainable systems, as it directly

influences the efficiency of energy systems and their environmental impact. The role of entropy in heat transfer and fluid dynamics becomes particularly significant when external factors like magnetic fields are altered. For example, Mehryan *et al*. [14] investigated the impact of variable magnetic fields on the flow and heat transfer properties of iron oxide nanoparticles in a container. They found that modifying the magnetic field could enhance both entropy and heat transfer efficiency, especially at high Rayleigh numbers. Furthermore, Huminic *et al*. [15] examined how hybrid nanofluids and nanofluids influence entropy generation, highlighting their potential as an innovative alternative to traditional thermal systems. Similarly, Khan and Alzahrani [16] explained the interactions of heat, magnetism, and particle motion to develop a mathematical model for Jeffrey nanofluid flow. Their model simplified complex mathematics to demonstrate how various parameters impact velocity, friction, and heat transport.

Further explorations into hybrid nanofluids were conducted by Akhter *et al*. [17] who investigated fluids composed of water mixed with copper and aluminium oxide nanoparticles in a heated chamber equipped with a heat-conducting cylinder, porous material, and a magnetic field. Their findings emphasized the effects of heat transport, magnetic field strength, nanoparticle composition, and porosity on fluid behaviour. Additionally, the creation of entropy in magnetized fluids over a stretched surface was studied using the Buongiorno model by Khan *et al*. [18], considering particle thermophoresis and diffusion. This study highlighted how factors such as radiation, magnetic fields, and fluid properties significantly affect entropy generation, temperature, and velocity. Moreover, using the Runge-Kutta method, Rafique *et al*. [19] investigated how nanoparticle shape affects heat transmission and entropy in water-alumina nanofluids, revealing that nanoparticles enhance heat transfer efficiency. Sharma *et al*. [20] focused on the interaction between solar radiation, nanoparticles, and microorganisms within a polyvinyl alcohol-water hydrogel in a parabolic trough solar collector, emphasizing heat transmission and entropy generation.

In the context of advanced technologies and industries, Ibrahim and Gamachu [21] explored the impact of varying nanoparticle concentrations of fluid flow and heat transfer on a rotating disc. By reducing entropy formation, performance is intended to be optimized. Meanwhile, Mahian *et al*. [22] studied the impact of nanofluids on heat transmission and entropy generation across different systems. Kumar *et al.* [23] investigated the impacts of magnetic fields and nanoparticle composition on entropy generation in nanofluid flow, with

particular implications for nuclear propulsion and spacecraft temperature control. Additionally, Rashidi *et al*. [24] investigated how a rotating porous disc responds to temperature and magnetic field variations. It finds that, for certain parameters, entropy creation is reduced, which suggests possible uses in renewable energy and space propulsion systems.

1.3 Swirling disk in fluid dynamics

In fluid dynamics, the concept of a "swirling disk" refers to a rotating disk3 that demonstrates the complex flow patterns of fluids around solid objects. This phenomenon is essential for understanding the intricate behaviours of fluids under rotational forces and has significant applications in various scientific and industrial fields. In hybrid nanofluids flow, analysis on swirling disks plays a crucial role. For instance, utilizing the Homotropy Analysis Method, Khan *et al*. [25] explored the fluid dynamics around a rotating disk, finding that an increase in coupling stress parameters results in decreased radial and axial velocities. This insight is crucial for the design of devices where fluid motion control is critical. Similarly, Beg *et al.* [26] developed a mathematical model for a device that integrates bacteria and nanoparticles, analyzing factors such as fluid flow, temperature, and motion. Their research holds potential for advancing technologies in food processing equipment by improving hygiene and efficiency.

Using mathematical models and simulations, Balaji *et al.* [27] examined the effects of magnetic and electrical fields on fluid flow and heat transfer, with real-world implications in coating operations, bioreactors, and medical sensors. Using the homotopy analysis method, Visuvasam and Alotaibi [28] studied Von Kármán swirling flows in a viscous liquid using the homotopy analysis method. They confirmed that stronger slide and hole effects significantly reduce fluid speed, aligning with computational predictions and enhancing our understanding of fluid dynamics in controlled environments. Similarly, Rana and Gupta [29] concentrated on the influence of heat and solute buoyancy forces in micro-liquid dynamics on a rotating disc. They discovered that thermophoresis significantly alters thermal behaviour, achieving optimal performance through advanced optimization techniques. Umavathi *et al*. [30] improved device design with more bacterial-resistant bio coatings by studying the dispersion of microbiological particles on rotating discs using nanotechnology and bioinspired approaches. Using graphs and

calculations to illustrate findings, Hussain *et al.* [31] investigated the effect of water-containing nanoparticles on heat transmission in a flexible disc under thermal radiation. Similarly, Tasawar and Hayat in [32] examined the constant movement of a viscous nanofluid in a porous media containing copper nanoparticles, examining variables such as heat radiation, slip, and viscous dissipation. The impact of radiation on fluid flow via a spinning disc is examined by Jain and Bohra [33] who utilized numerical techniques and graphic analysis to investigate the impact of radiation on fluid flow through a spinning disc. Their analysis of temperature and velocity variations under different fluid parameters provides valuable data for improving industrial processes involving rotational flow dynamics. Using numerical techniques, Zhang *et al*. [34] discovered that a wavy, rotating disc improves thermal energy transfer in a water-based nanofluid containing nanoparticles of magnesium oxide and silver. Additionally, Attia *et al*. [35] explored the impact of porosity temperature and velocity patterns. This study investigated the fluid flow over a rotating disc in a porous medium using numerical techniques, to examine the impact of medium permeability on heat transfer and fluid flow.

1.4 Thesis Contributions

In this thesis, a detailed review of the work of Attia *et al.* [35] is presented. Furthermore, this study presents the extension to base study by investigating how porous media and viscous dissipation impact the steady flow and heat transfer over a swirling disk. The primary objective is to use the von Kármán transformation to convert the complex partial differential equations (PDEs) into ordinary differential equations (ODEs). The transformed equations are then solved by using MATLAB's bvp-4c solver. Detailed results and discussions are presented through both graphical and tabular formats, enhancing the understanding of fluid behaviour in engineered porous structures and contributing significantly to the field of fluid dynamics.

1.5 Thesis Organization

This thesis is divided into multiple chapters, and the details of each chapter are as follows:

Chapter 1 is an introductory chapter and provides a brief overview of the important concepts, brief literature on hybrid nanofluids, thesis contributions and organization.

Chapter 2 offers essential definitions, guidelines, and concepts necessary to realize upcoming work. The mathematical model and shooting method are mentioned on the concluding page of this chapter.

Chapter 3 offers a detailed review of the works done by Attia *et al*. [35] and provide the simulation of baseline work for comparison.

Chapter 4 presents the extended work of Attia *et al*. [35] the numerical investigation of the consequences of entropy generation in an Al_2O_3/Methanol nanofluid flowing across a rotating disc. The main objective is to study the heat transfer dynamics and steady-state incompressible flow characteristics of the nanofluid. The bvp-4c solver in MATLAB is then used to solve these modified equations. The findings, which show how these parameters affect entropy generation and thermal performance, are displayed as graphs and tables.

Chapter 5 provides the conclusion of this thesis and highlights the future research direction.

References In the end, a list of references is given for use in this study.

CHAPTER 2

BASIC DEFINITIONS

This chapter includes several common definitions, terms, and rules used in the thesis to help readers comprehend the formal results and analysis done in the study.

2.1 Fluid

Fluid is defined as a liquid substance that can flow and fit the shape of its container under applied shear stress. It includes both liquids and gases and differs from solids in its inability to resist deformation persistently. Fluids are characterized by properties such as viscosity, which describes their resistance to flow; compressibility, which indicates how much they can be compacted; and density, which is their mass per unit volume. These properties make fluids integral to understanding and analyzing phenomena in fields like hydraulics, meteorology, and various engineering disciplines.

2.1.1 Fluid Mechanics

It is a branch of physics that studies the behaviour of fluids, which includes liquids, gases, and plasmas, as well as the forces acting on them. It also includes fluid statics, which deals with the study of fluids at rest, and also with fluid dynamics, which studies fluids in motion. This field is fundamental in understanding and designing systems in which fluids are in motion or at rest, such as in aerodynamics, hydrodynamics, weather systems, and many engineering applications.

2.1.2 Fluid Dynamics

Fluid dynamics, which focuses on the study of fluids in motions is a sub-discipline of fluid mechanics. It involves analyzing the behaviour and properties of liquids and gases in motion, covering various phenomena such as flow velocity, pressure, density, and temperature changes. This field is crucial for solving practical problems in engineering and science, including designing aircraft and vehicles for optimal aerodynamics, understanding weather patterns, engineering efficient water supply systems, and exploring complex biological flows such as blood circulation.

2.2 Physical Properties of the fluid

2.2.1 Pressure

Pressure in physics is defined as the force per unit area exerted perpendicular to the surface. Generally, it is expressed in terms of units such as pascals (Pa), atmospheres (atm), or pounds per square inch (psi). The mathematical expression for pressure is given as:

$$P = \boldsymbol{F}/A, \tag{2.1}$$

where P, F and A represent pressure, force, and area, respectively**.**

2.2.2 Density

Density, which is a measurement of mass per unit volume of a material or substance, indicates how much mass is present in a specific volume and is stated in quantities like grammes per cubic centimeter (g/cm^2) or kilograms per cubic metre (kg/m^3).

$$\rho = m/v. \tag{2.2}$$

2.2.3 Temperature

Temperature is a fundamental physical quantity that measures the average kinetic energy of the particle, indicating how cold or hot an object is. This measure plays a crucial role in determining the physical state (solid, liquid, gas) of a substance. The temperature is usually measured in either Fahrenheit (°F), degrees Celsius (°C), or Kelvin (K). In the context of physics and chemistry, temperature influences a wide range of material properties and behaviors, including phase transitions (like melting and boiling), reaction rates, and the expansion or contraction of materials. It is also a key parameter in the laws of thermodynamics, which describe heat transfer between systems.

2.2.4 Dynamic Viscosity

Viscosity is a property of fluids which describes the resistance of fluid flow and internal friction. It indicates how much a fluid resists being deformed by shear or tensile stress. There are two types of viscosity, in which dynamic viscosity measures the force needed to slide one layer of fluid over another, and kinematic viscosity, which considers the fluid's density in its calculation. Mathematically, viscosity is given as:

$$\text{Viscosity} = \mu = \frac{\text{shear stress}}{\text{rate of sheare strain}} . \qquad (2.3)$$

2.2.5 Kinematic Viscosity

Kinematic viscosity measures the resistance to fluid flow and diffusion under the influence of gravitation force. It is the ratio of the density and fluid's dynamic viscosity. Kinematic viscosity indicates how quickly a fluid will spread out or diffuse in the absence of any external force other than gravity. The unit of kinematic viscosity is Stoke (St) or meters squared per second (m^2/s), where one stokes equals 10^{-4} m^2/s.

2.2.6 Stress

Stress in a physical context refers to the internal force exerted by one part of an object on another part per unit area. It arises when external forces are applied to a material or when internal forces are induced by influences such as temperature changes or deformation. Stress is typically measured in units of pressure, such as pascals (Pa) or pounds per square inch (psi).

2.2.7 Shear Stress

Shear stress occurs when a force is applied parallel to the surface of a material, causing layers to slide relative to each other. This action is distinct from tensile or compressive stress, where the forces are perpendicular to the surface of the material,

$$\boldsymbol{\tau} = \boldsymbol{F}/A\ , \tag{2.4}$$

where $\boldsymbol{F}$ noted the force and A represent area.

2.2.8 Normal Stress

Normal stress is defined as the internal force per unit area (stress) generated by forces like tension or compression within a material and perpendicular to its surface.

2.2.9 Newton's Law of Viscosity

This law defines the connection between the shear stress and the rate of strain (or velocity gradient) in a fluid. It states that for many fluids, the shear stress between adjacent fluid layers is proportional to the rate at which the layers move relative to each other. Mathematically, it is expressed as:

$$\tau_{xy} \propto \frac{\partial u}{\partial y}\,, \tag{2.5}$$

or

$$\tau_{xy} = \mu\left(\frac{\partial u}{\partial y}\right). \tag{2.6}$$

According to this law, fluids that exhibit this relation are terms as true are known as Newtonian fluids. The most common examples of such Newtonian fluids are water, air, and light oils, where the viscosity remains constant regardless of the forces applied. This law is foundational in fluid mechanics, helping to explain and predict the flow behavior of fluids under various conditions.

2.3 Types of fluid flow

2.3.1 Flow

A fluid or gas moves continuously through a conduct or across a surface under the influence of gravity, pressure differentials, or other external factors. Its direction and rate are what define the flow**.**

2.3.2 Compressible Flow

When a fluid flows at a high speed or at a different temperature, it is said to be compressible because the fluid density substantially reacts to pressure changes. For example, it flows over an aircraft wing at high speed.

2.3.3 Incompressible Flow

Incompressible flow refers to a fluid flow condition where the fluid density remains constant, even with changes in pressure or flow velocity. This condition is commonly assumed for liquids and low-speed gas flows, such as water flowing through a household plumbing system.

2.3.4 Steady Flow

When there is steady flow, there are no time-varying changes in the fluid's velocity, pressure, or other flow characteristics at any one site,

$$\frac{\partial \lambda}{\partial t} = 0, \tag{2.7}$$

where λ is any fluid property. For example, the flow of water in a pipe.

2.3.5 Unsteady Flow

When a fluid's velocity varies over time, the flow is said to be unsteady because its direction and speed fluctuate instead of staying constant,

$$\frac{\partial \lambda}{\partial t} \neq 0, \tag{2.8}$$

For example, pulsatile blood flow in arteries and exhaust from an accelerating vehicle.

2.3.6 Laminar Flow

Fluid motion, known as laminar flow, produces a clean and organised flow pattern when the fluid moves in parallel layers without interruption**.** For example, honey flows from a Spoon, and blood flows in capillaries.

2.4 Type of Fluids

2.4.1 Ideal Fluid

An ideal fluid is a hypothetical substance that is viscosity-free and incompressible, implying that it does not encounter internal friction or flow resistance. For example, air is used in theoretical aerodynamics, and water is used in basic hydrodynamics.

2.4.2 Real Fluid

A real fluid, also called a viscous fluid, behaves differently from an ideal fluid, particularly when stress is applied. Their viscosity gives them resistance to deformation and flow. For example, oil is used in engine lubrication, and blood is used in the human circulatory system.

2.4.3 Newtonian Fluid

In a Newtonian fluid, the local strain rate corresponds to the rate at which the fluid's deformation changes over time, and the viscous stresses resulting from its flow are consistently proportional at all points in time. This indicates that regardless of the load placed on it, its viscosity is constant. For example, water, air, mineral oils, glycerin.

2.4.4 Non- Newtonian Fluid

A non-Newtonian fluid is one whose viscosity, as opposed to the constant viscosity of Newtonian fluids, varies in response to stress or shear. It may thicken or thin. For example, ketchup, toothpaste, blood.

2.4.5 Nano-Fluid

A nanofluid refers to a fluid that contains suspended nanoparticles that enhance its thermal conductivity and heat transfer properties due to the small size of the particles. For example, cooling fluids in electronics and heat transfer fluids in solar collectors.

2.5 Heat Transfer Mechanism and Properties

2.5.1 Heat Transfer

The process through which thermal energy is moved across physical systems is known as heat transfer. The method depends on the temperature differential and the characteristics of the medium used to transfer the heat. The following are the ways through which the heat is transferred.

2.5.2 Conduction

When there is a temperature or electrical potential differential between adjacent regions, a substance can transfer heat or electricity directly through it without moving. This phenomenon is known as conduction. For example, a classic example of conduction, the process by which heat passes from the iron to your skin, is touching a hot iron and feeling it transfer straight to your hand.

2.5.3 Convection

Convection is the movement of heat through a fluid (liquid or gas) due to molecular motion. Warmer fluid particles rise to the surface while colder particles sink, resulting in a circulating pattern. For example, convection is demonstrated by a pot of boiling water on the stove, where heat moves through the water, pushing hotter water to the top and colder water to the bottom.

2.5.4 Radiation

The transfer of energy without the need for physical contact through space or a medium in the form of electromagnetic waves or particles is known as radiation.

2.6 Viscous Dissipation

The process of internal friction in a fluid flow transforms mechanical energy into heat, which is known as viscous dissipation.

$$\Phi = \mu \Sigma \left(\frac{\partial u_i}{\partial x_j} + \frac{\partial u_j}{\partial x_i} \right), \tag{2.9}$$

where Φ is viscous dissipation, μ is dynamic viscosity, u_i and u_j are the components of the fluid in the respective x_j and x_i direction.

2.7 Thermal Conductivity

A material's thermal conductivity measures its ability to conduct heat. It is defined as the amount of heat passing through a unit area of the material in a unit of time under a unit temperature gradient.

$$k = \frac{Q \,.\, L}{A \,.\, \Delta T} \,. \tag{2.10}$$

2.8 Thermal Diffusivity

A substance's thermal diffusivity, or the rate at which heat diffuses through it, tells us how rapidly a material reacts to temperature changes.

$$\alpha = \frac{k}{\rho \,.c_p}. \tag{2.11}$$

2.9 Mixed Convection

The process of heat transmission, known as "mixed convection," occurs when a fluid is concurrently subjected to forced convection (caused by external forces like a pump or fan) and natural convection (caused by buoyant forces).

2.10 Solution of Methodology

One numerical method for solving boundary value problems (BVPs) for ODEs is known as the shooting method. It works especially well with second-order differential equations, but it can also be modified to work with higher-order problems. This technique converts a boundary value problem into its corresponding initial value problem (IVP) so that common techniques such as Runge-Kutta can be applied to solve it [36].

$y'' = f(x, y, y')$, with $y(a) = \alpha \ and \ y(b) = \beta,$ (2.12)

The solutions to two initial-value problems cannot be combined linearly to form a nonlinear problem. These issues take the following form:

$y'' = f(x, y, y'), \ \ with \ y(a) = \alpha \ and \ y'(a) = t$, (2.13)

by choosing the parameters t

$$\lim_{k\to\infty}(b = t_k), = y(b) = \beta, \quad (2.14)$$

where $y(x, t_k)$ denotes the IVP of (2.12) with $t = t_k$, and $y(x)$ denotes the solution to the problem (2.11). A variable t_0 indicates the starting height at which the item is launched from the point (a, α) along with the curve that the IVP solution describes:

$y'' = f(x, y, y')$, with $y(a) = \alpha \ and \ y'(a) = t_0,$ (2.15)

We adjust our approximation by selecting heights t_1, t_2, until $y(b, t_k)$ is close to "hitting" β if $y(b, t_0)$ is not close enough.

$$y(b, t) - \beta = 0 . \quad (2.16)$$

The problem can be solved using the second technique by first selecting the initial approximations, t_0 and t_1, and then generating the remaining terms in the sequence by

$$t_k = t_{k-1} - \frac{(y(b,t_{k-1})-\beta)(t_{k-1}-t_{k-2})}{y(b,t_{k-1})-y(b,t_{k-2})}, \qquad k = 2,3,\ldots\ldots \quad (2.17)$$

There is just one initial approximation, t_0, required to construct the sequence (t_k) using the more potent Newton's approach.

$$t_k = t_{k-1} - \frac{y(b,t_{k-1})-\beta}{\frac{dy}{dt}(b,t_{k-1})}, \quad (2.18)$$

and it necessitates an understanding of $(dy/dt)(b, t_{k-1})$. This is a challenge since we only know the values $y(b, t_0), y(b, t_1), \ldots, y(b, t_{k-1})$; an explicit representation for $y(b, t)$ is unknown.

Let's say we reword the initial-value problem (2.12) to highlight the fact that the parameter t and x are both necessary for the solution to occur:

$$y''(x,t) = f\left(x, y(x,t), y'(x,t)\right), \text{ with } \quad y(a,t) = \alpha \quad \text{and} \quad y(a,t) = t. \tag{2.19}$$

To denote differentiation with respect to x, we have kept the prime notation. When $t = t_{k-1}$, we must calculate $(\frac{dy}{dt})(b,t)$, thus, we start by taking the partial derivative of (2.17) with respect to t. This suggests that:

$$\frac{\partial y''}{\partial t}(x,t) = \frac{\partial f}{\partial t}(x, y(x,t), y'(x,t)) \,. \tag{2.20}$$

x and t are the independent variable, so $\frac{\partial x}{\partial t} = 0$ and simplify Eq. (2.19)

$$\frac{\partial y''}{\partial t}(x,t) = \frac{\partial f}{\partial y}(x, y(x,t), y'(x,t))\frac{\partial y}{\partial t}(x,t)) + \frac{\partial f}{\partial y'}(x, y(x,t)) \,. y'(x,t))\frac{\partial y'}{\partial t}(x,t) \,, \tag{2.21}$$

The initial conditions are

$$\frac{\partial y}{\partial t}(a,t) = 0 \,, \tag{2.22}$$

and

$$\frac{\partial y'}{\partial t}(a,t) = 1. \tag{2.23}$$

If we suppose that the order of differentiation of x and t can be reversed and simplify the notation by using $z(x,t)$ to denote$\frac{\partial y'}{\partial t}(x,t)$ then (2.17) with the initial conditions becomes the initial-value problem,

$$z''(x,t) = \frac{\partial f}{\partial y}(x, y, \acute{y})z(x,t) + \frac{\partial f}{\partial y'}(x,t), \tag{2.24}$$

$$\text{with } \; z(a,t) = 0 \quad \text{and} \quad z(a,t) = 1.$$

Newton's method requires two initial-value problems so (2.17) and (2.22) to solve each iteration

$$t_k = t_{k-1} - \frac{y(b,t_{k-1}) - \beta}{z(b,t_{k-1})}. \tag{2.25}$$

2.11 Continuity Equation

The continuity equation explains the principle of conservation of mass in fluid dynamics. It states that the rate at which mass enters the system is equal to the rate at which it exits, plus the rate of accumulation within the system,

$$\frac{\partial \rho}{\partial t} + \boldsymbol{\nabla}.(\rho.\boldsymbol{V}) = 0\,, \tag{2.26}$$

For incompressible flow,

$$\boldsymbol{\nabla}.\boldsymbol{V} = 0\,. \tag{2.27}$$

2.12 Momentum Equation

The momentum equation in fluid dynamics describes the conservation of momentum for a fluid element. It is frequently derived from Newton's second law of motion. The equation links the external forces acting on the fluid to the rate of change of momentum within the flow field. It is crucial for predicting forces and fluid motion.

$$\rho(\boldsymbol{V}.\ \boldsymbol{\nabla})\boldsymbol{V} = -\boldsymbol{\nabla}p + \mu\boldsymbol{\nabla^2}\,\boldsymbol{V} + \rho\boldsymbol{b}, \tag{2.28}$$

where ρ is the fluid density, p is the pressure, μ is the dynamic viscosity b is the body force.

2.13 Energy Equation

The energy equation is a mathematical statement that explains the idea of energy conservation. It states that the energy of an isolated system remains constant throughout time and is frequently used in the context of physics and engineering. It usually manifests as kinetic energy plus potential energy equals constant, which captures the transformation of one form of energy into another but excludes the generation or destruction of new forms of energy.

$$(\rho c_p)(\boldsymbol{V}.\boldsymbol{\nabla})T = k\boldsymbol{\nabla^2}\,T + \Phi, \tag{2.29}$$

where T is the temperature, k is thermal conductivity, and Φ is viscous dissipation.

2.14 Dimensionless Parameter

2.14.1 Prandtl number (Pr)

The ratio of thermal diffusivity to momentum diffusivity, or kinematic viscosity, determines the Pr, a dimensionless quantity that expresses the relative thickness of the thermal and momentum boundary layers in a fluid flow.

$$Pr = \frac{\upsilon}{\alpha} = \frac{\mu c_p}{k}. \tag{2.30}$$

2.14.2 Eckert number (Ec)

The ratio of kinetic energy to enthalpy difference, or "*Ec*," is a dimensionless number used in fluid dynamics. It typically illustrates the link between a flow's kinetic energy and the energy needed to raise a fluid's temperature. It is frequently employed to measure how much kinetic energy in a flow is converted to thermal energy,

$$Ec = \frac{u^2}{c_{p\Delta T^2}}. \tag{2.31}$$

u is the velocity flow, c_p is the specific heat.

2.14.3 Skin Friction (c_f)

The force of resistance that exists between the surface of a solid object moving through a fluid, such as water or air, is called skin friction. Mathematically, it is defined as

$$c_f = \frac{\tau_w}{\frac{1}{2}\rho u^2}, \tag{2.32}$$

where shear stress is depicted as τ_w , density is denoted by ρ and u represents the free-stream velocity.

2.14.4 Nusselt Number (Nu)

The Nusselt number quantifies the ratio of convective to conductive heat transfer at a boundary. Mathematically, it is defined as

$$Nu = \frac{h\Delta T}{K\frac{\Delta T}{L}} = \frac{hL}{k}, \tag{2.33}$$

where h is the temperature transfer due to convection, L is the specific length, ΔT is the temperature difference, and k denotes the fluid's thermal conductivity.

2.14.5 Bejan Number *(Be)*

The Bejan number *(Be)* is a dimensionless quantity which quantifies the ratio of fluid friction irreversibility to heat transfer irreversibility in a flow process.

$$Be = \frac{\text{Pressure drop irreversibility}}{\text{Total irreversibility}}. \tag{2.34}$$

2.14.6 Brickmann Number *(Br)*

The Brinkman number *(Br)* measures the ratio of viscous dissipation to conductive heat transfer within a fluid. This dimensionally less quantity is particularly relevant in the study of heat transfer in fluid flow, especially in cases where viscous heating is significant, such as in high-speed or highly viscous flows.

$$Br = \frac{\mu U^2}{k(T_w - T_\infty)}, \tag{2.35}$$

where U is the velocity of the fluid, μ is dynamic viscosity and k is thermal conductivity.

CHAPTER 3

STEADY FLOW OVER A ROTATING DISK IN A POROUS MEDIUM WITH HEAT TRANSFER

3.1 Overview

This section studies the flow and heat transfer of an incompressible viscous fluid over an infinite rotating disk in a porous media. Numerical methods are used to find the solution. The impact of the medium's porosity on the temperature and velocity distributions is considered. The results are given in the form of graphs and tables.

3.2 Mathematical Formulation

Let the disk be in the plane z = 0 and suppose that a viscous incompressible fluid fills the space z > 0. The motion is caused by an infinitely large, insulated disk rotating at a constant angular speed ω through a porous mate, which presents the impact of the porosity of the medium on steady flow and heat transfer. The disk is rotated about an axis orthogonal to its plane. If not, the fluid is under pressure (p_∞) and at rest.

The velocity field $\boldsymbol{V}$ in cylindrical coordinates (r, ϕ, z) is described by the components:

$$\boldsymbol{V} = [u(r,z), v(r,z), w(r,z)] , \tag{3.1}$$

where *u*, *v*, and *w* represent the velocity components in the *r*, ϕ and *z* directions. The governing equations for the incompressible, steady-state flow include the continuity and Navier-Stokes equations modified for a porous medium.

$$\boldsymbol{\nabla} . \boldsymbol{V} = 0 . \tag{3.2}$$

$$\rho(\boldsymbol{V}.\nabla)\boldsymbol{V} = -\boldsymbol{\nabla}\mathrm{P} + \mu\boldsymbol{\nabla^2 V} - \frac{\mu}{k}\boldsymbol{V}\,, \tag{3.3}$$

and

$$(\rho c_p\,)(\boldsymbol{V}.\boldsymbol{\nabla})T = k\boldsymbol{\nabla^2}\,T + \Phi. \tag{3.4}$$

The component form of the constitutive equations are given below;

$$\frac{\partial u}{\partial r} + \frac{u}{r} + \frac{\partial w}{\partial z} = 0, \tag{3.5}$$

$$\rho\left(u\frac{\partial u}{\partial r} + w\frac{\partial u}{\partial z} - \frac{v^2}{r}\right) + \frac{\partial p}{\partial r} = \mu\left(\frac{\partial^2 u}{\partial r^2} + \frac{1}{r}\frac{\partial u}{\partial r} - \frac{u}{r^2} + \frac{\partial^2 u}{\partial z^2}\right) - \frac{\mu}{K}u, \tag{3.6}$$

$$\rho\left(u\frac{\partial v}{\partial r} + w\frac{\partial v}{\partial z} + \frac{uv}{r}\right) = \mu\left(\frac{\partial^2 v}{\partial r^2} + \frac{1}{r}\frac{\partial v}{\partial r} - \frac{v}{r^2} + \frac{\partial^2 v}{\partial z^2}\right) - \frac{\mu}{K}v, \tag{3.7}$$

$$\rho\left(u\frac{\partial \mathrm{w}}{\partial \mathrm{r}} + w\frac{\partial \mathrm{w}}{\partial \mathrm{z}}\right) + \frac{\partial \mathrm{p}}{\partial \mathrm{z}} = \mu\left(\frac{\partial^2 \mathrm{w}}{\partial \mathrm{r}^2} + \frac{1}{\mathrm{r}}\frac{\partial \mathrm{w}}{\partial \mathrm{r}} + \frac{\partial^2 \mathrm{w}}{\partial \mathrm{z}^2}\right) - \frac{\mu}{\mathrm{K}}w\,, \tag{3.8}$$

and

$$\rho \mathrm{c_p}\left(u\frac{\partial \mathrm{T}}{\partial \mathrm{r}} + w\frac{\partial \mathrm{T}}{\partial \mathrm{z}}\right) = \mathrm{k}\left(\frac{\partial^2 \mathrm{T}}{\partial \mathrm{z}^2} + \frac{\partial^2 \mathrm{T}}{\partial \mathrm{r}^2} + \frac{1}{\mathrm{r}}\frac{\partial \mathrm{T}}{\partial \mathrm{r}}\right) + \mu[\left(\frac{\partial u}{\partial \mathrm{z}}\right)^2 + \left(\frac{\partial v}{\partial \mathrm{z}}\right)^2. \tag{3.9}$$

with the boundary condition

$$u = 0,\ v = \omega r,\ w = 0\,,\ T = T_w\ at\ z = 0, \tag{3.10}$$

$$u \to 0,\ v \to 0,\ p \to p_{\infty,}\ T \to T_\infty\ \ as\ z \to \infty, \tag{3.11}$$

where p stands for pressure, μ for viscosity, ρ for fluid density and K for Darcy permeability. The velocity components u, v, and w are in the direction of increasing r, ϕ, and z, respectively. Von Karman transformation is defined below;

$$u = r\omega F(\xi),\quad v = r\omega G(\xi),\ w = \sqrt{\omega\nu}\,H(\xi)\,,\quad z = \frac{\sqrt{\nu}}{\omega}\xi\,,\ p - p_\infty = -p\nu\omega P\,,\quad \text{and}$$

$$\theta = \frac{T - T_\infty}{T_w - T_\infty}, \tag{3.12}$$

where ν is the fluid's kinematic viscosity, ξ denotes the non-dimensional distance along the axis of rotation. F, G, H, and P denotes non-dimensional functions of ξ.

$$\frac{dH}{d\xi} + 2F = 0\,, \tag{3.13}$$

$$\frac{d^2F}{d\xi^2} - H\frac{dF}{d\,\xi} - F^2 + G^2 - MF = 0\,, \tag{3.14}$$

$$\frac{d^2G}{d\,\xi^2} - H\frac{dG}{d\xi} - 2FG - MG = 0\,, \tag{3.15}$$

$$\frac{d^2H}{d\xi^2} - H\frac{dH}{d\xi} + \frac{dP}{d\xi} - MH = 0\,, \tag{3.16}$$

and

$$\frac{1}{Pr}\frac{d^2\theta}{d\xi^2} - H\frac{d\theta}{d\xi} + Ec\,[\left(\frac{dF}{d\xi}\right)^2 + \left(\frac{dG}{d\xi}\right)^2] = 0\,. \tag{3.17}$$

The porosity parameter is $M = \nu/K\omega$, Prandtl number is $Pr = c_p\mu/k$ and Eckert number is $Ec = \frac{r^2\omega^2}{c_{p(T_w - T_\infty)}}$.

With dimensionless boundary conditions ;

$$F = 0\,, G = 1\,,\ H = 0 \quad \text{when} \quad \xi = 0\,, \tag{3.18}$$

$$F \to 0\,, G \to 0, \quad p \to 0 \quad \text{when } \xi \to \infty\,, \tag{3.19}$$

and

$$\theta(0) = 1,\ \theta(\infty) = 0. \tag{3.20}$$

These equations and boundary conditions describe the fluid flow behavior and heat transfer over a rotating disk in a porous medium. The system of partial differential equations is solved using numerical methods to obtain the velocity and temperature distributions. The obtained solutions then analyze the impact of the medium's porosity on the fluid dynamics and thermal characteristics.

3.3 Methodology

The set of nonlinear ordinary differential equations (ODEs) derived from Eq. (3.13)-(3.17), with boundary conditions (3.18)-(3.20), are solved using the built-in bvp4c of MATLAB software to solve dimensionless boundary value problems for ODE. The mathematical solution for the converted system is defined as follows:

$x_1 = F$, $x_2 = F'$, $x_3 = G$, $x_4 = G'$, $x_5 = H$, $x_6 = \theta$, $x_7 = \theta'$ as follows:

$x_1{}' = x_2,$ $x_1(0) = 0$,

$x_2{}' = x_5 x_2 - x_3^2$, $x_2(0) = s^{(1)}$,

$x_3{}' = x_4$, $x_3(0) = 1$,

$x_4{}' = x_5 x_4 + 2x_1 x_3$, $x_4(0) = s^{(3)},$

$x_5{}' 2x_1$, $x_5(0) = 0,$

$x_6{}' = x_7$, $x_6(0) = 1,$

$x_7{}' = (\mathrm{Pr}) x_5 x_7 - PrEc(x_2^2 + x_4^2),$ $x_4(0) = s^{(6)},$

where s^1, s^3 and s^6 are chosen to be $x_1(\infty) = 0, x_3(\infty) = 0$, $x_6(\infty) = 0$. The width of the boundary layer in the given equation is represented by "infinity".

The solutions obtained using this method are validated by comparing them with previous studies. For example, the results of a typical Newtonian fluid match closely with the findings of Rashidi *et al.* [24]. Additionally, the velocity profile values provided in Table 3.1 correspond precisely with the reference values, confirming the accuracy of the numerical method employed [24].

Table 3.1: Values of $F'(0)$, $G'(0)$, $\theta'(0)$ compared with Rashidi et al. [24]

$F'(0)$		$G'(0)$		$\theta'(0)$	
Rashidi *et al* [24]	presented	Rashidi *et al* [24]	presented	Rashidi *et al* [24]	Presented
0.510233	0.510186	0.61592	0.61589	0.32586	0.3276

The numerical solution to the differential equations for the considered fluid model along with the boundary conditions is obtained by employing the built-in bvp4c technique in MATLAB software. This approach allows for the accurate and efficient determination of the velocity and temperature distributions in the flow over a rotating disk in a porous medium, considering the effects of porosity on the system. The numerical solutions obtained provide valuable insights into the fluid dynamics and heat transfer characteristics of the system under study.

3.4 Results and Discussion

This chapter presents the impact of variation in porosity parameter M and Prandtl number Pr on velocity profiles and temperature. For instance, the results in Figure 3.1 present the effects of the porosity of the medium on the flow of velocity in the radial direction. The results indicate that the increase in the porosity parameter M will decrease F and the thickness of the boundary layer. The variations in the velocity component G's profile are shown in Figure. 3.2 for different values of M. The results show how the porosity of the medium affects the tangential velocity G. The momentum boundary layer thickness decreases as the porosity parameter M rises. Figure 3.3 illustrates variations in the profile of the velocity component H as the value of the porosity parameter varies. As the porosity parameter M increases, the axial velocity component H and, hence, the thickness of the momentum boundary layer both increase. Additionally, increasing the porosity parameter will affect the viscous forces more significantly, which results in a decrease in the velocity profile.

The results in Figure 3.4 present the influence of the porosity parameter M on the temperature θ. This is because the porosity prevents the fluid at almost ambient temperature from reaching the disk's surface. As a result, raising M raises both the temperature and the thickness of the thermal boundary layer. Heat transmission is increased at the surface when no fluid is present and the temperature is close to ambient. In Figure 3.5, it is observed that by increasing the Prandtl number Pr, the thermal boundary layer decreases.

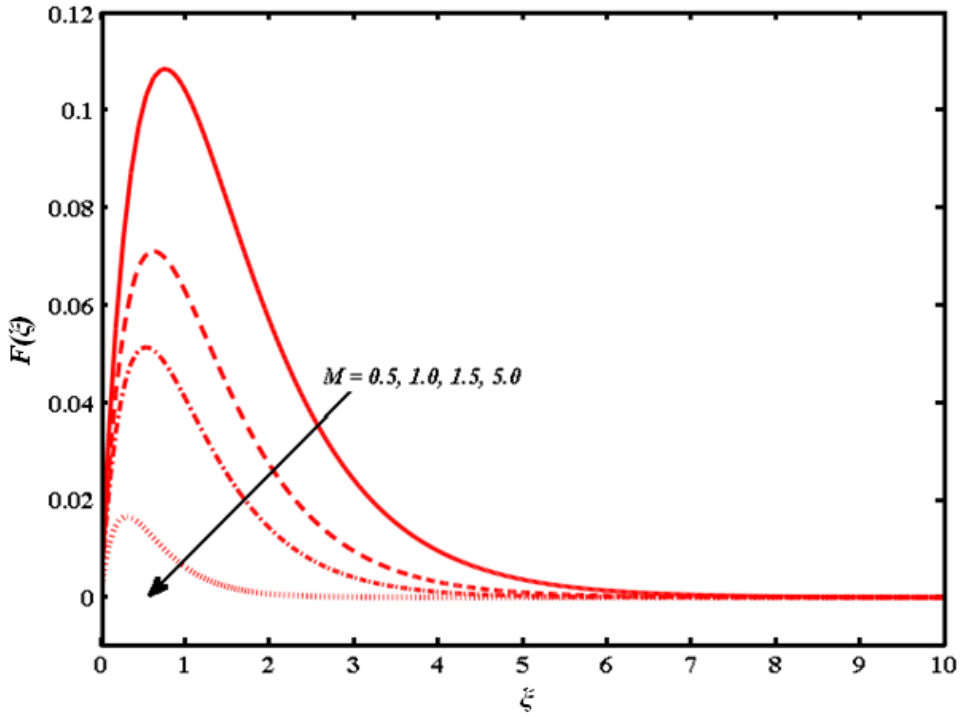

Figure 3.1: Effect of porosity parameter M on the radial velocity profile $F(\xi)$.

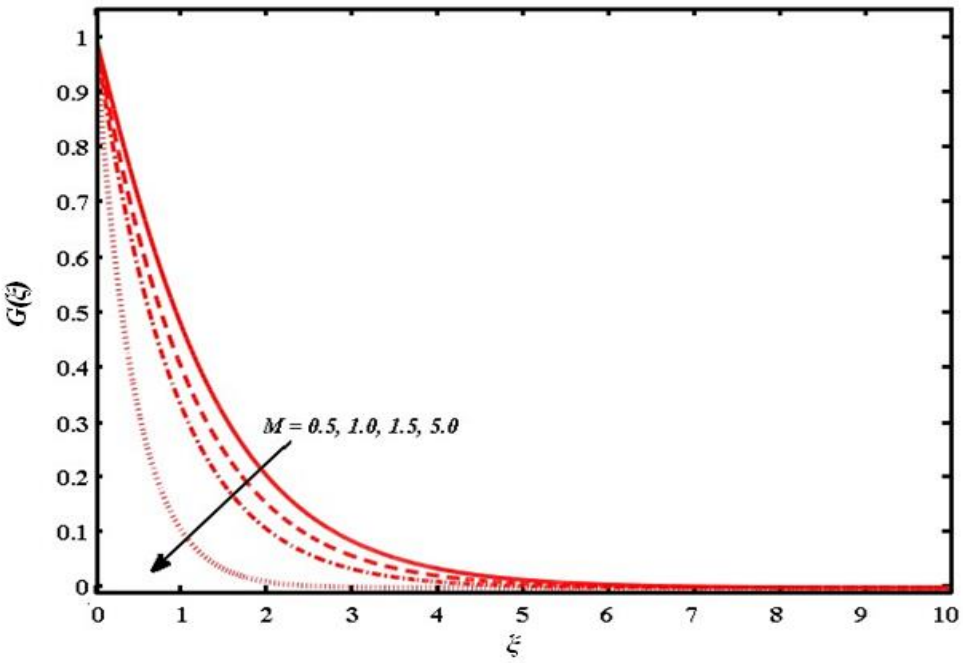

Figure 3.2: Effect of the porosity parameter M on the tangential velocity profile $G(\xi)$.

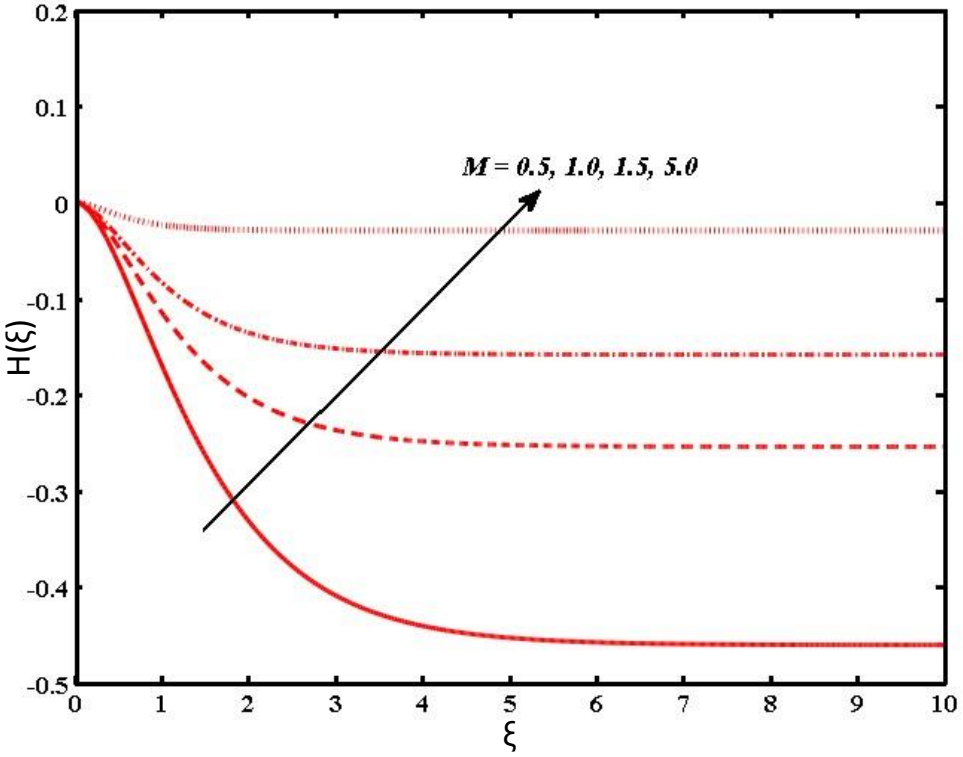

Figure 3.3: Effect of the porosity parameter M on the axial velocity profile $H(\xi)$**.**

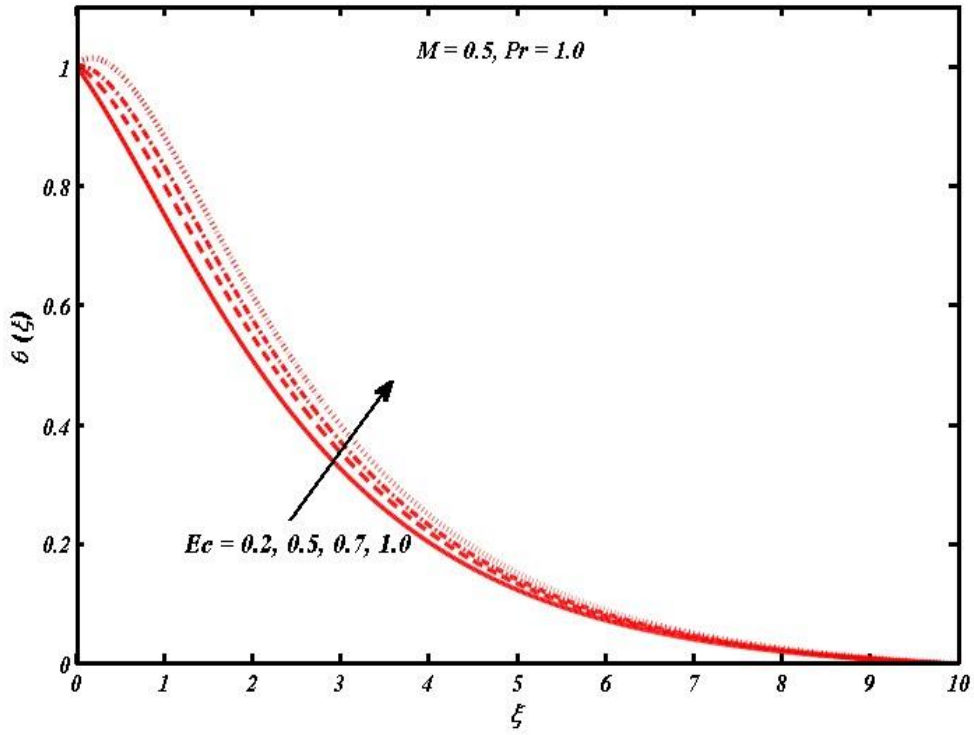

Figure 3.4: Effect of Eckert number on the temperature profile of $\theta(\xi)$.

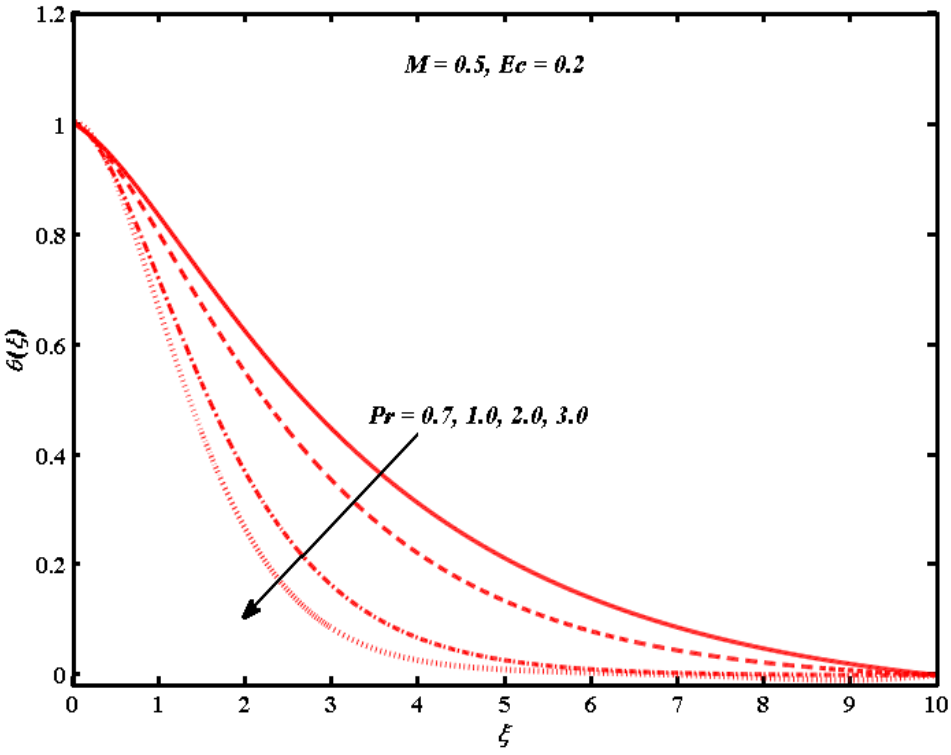

Figure 3.5: Effect of the *Pr* number on the temperature profile $\theta(\xi)$.

CHAPTER 4

NUMERICAL STUDY OF ENTROPY GENERATION EFFECT IN Al_2O_3/METHANOL NANOFLUID FLOWS OVER A SWIRLING DISK

4.1 Introduction

In this section, we have considered the base fluid Methanol, and the nanoparticle is Al_2O_3. The fluid is flowing over the surface of the swirling disk, and entropy generation is being examined. The problem is then mathematically formulated, and the main PDEs are converted into nonlinear ODEs. Transformed equations are solved mathematically. The results obtained are discussed briefly through graphs and tables. The effects of several related constraints, such as, C_f and Nu , N_s, Be and Br on the velocity profile $F(\xi)$ and temperature profiles $\theta(\xi)$ are displayed through graphs.

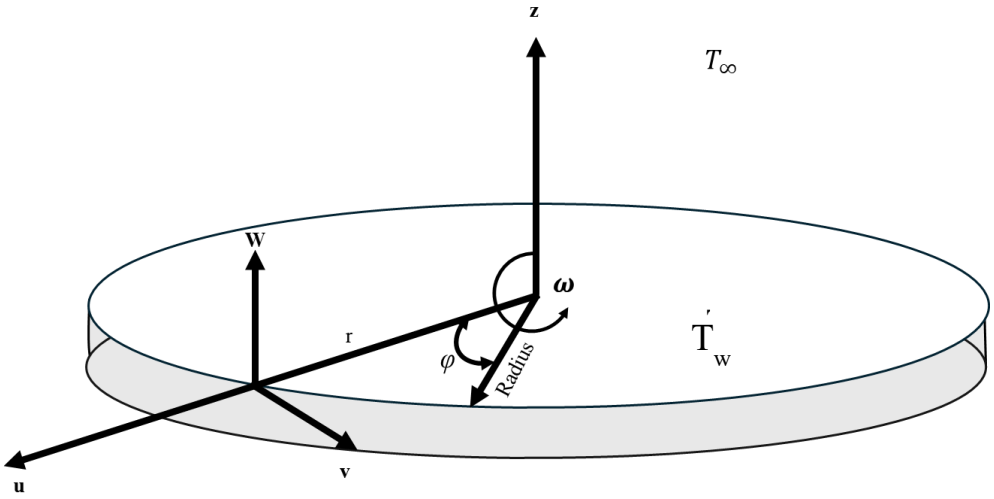

Figure 4.1: Physical representation of the problem.

4.2 Mathematical formulation

Suppose a steady, incompressible flow of nanofluid over a rotating disk. The base fluid comprises of Methanol, and the nanoparticles suspended in it are Al_2O_3. Let the disc be in the plane z = 0, and suppose the incompressible nanofluid fills the space z > 0. The equations for the flow and heat transfer in cylindrical coordinates can be expressed as:

The velocity field of the equation is given as below;

$$\boldsymbol{V} = [u(r,z), v(r,z), w(r,z)] , \tag{4.1}$$

The equations of motion for incompressible steady flow defined as below;

$$\boldsymbol{\nabla} . \boldsymbol{V} = 0, \tag{4.2}$$

$$\rho_{nf}(\boldsymbol{V}.\boldsymbol{\nabla})\boldsymbol{V} = -\boldsymbol{\nabla}P + \mu_{nf}\boldsymbol{\nabla^2}\boldsymbol{V} , \tag{4.3}$$

and

$$(\rho c_p)_{nf}(\boldsymbol{V}.\boldsymbol{\nabla})T = k_{nf}\boldsymbol{\nabla^2}\, T + \Phi . \tag{4.4}$$

The component form of the constitutive equations are given below:

$$\frac{\partial u}{\partial r} + \frac{u}{r} + \frac{\partial w}{\partial z} = 0, \tag{4.5}$$

$$\rho_{nf}\left(u\frac{\partial u}{\partial r} + w\frac{\partial u}{\partial z} - \frac{v^2}{r}\right) + \frac{\partial p}{\partial r} = \mu_{nf}\left(\frac{\partial^2 u}{\partial r^2} + \frac{1}{r}\frac{\partial u}{\partial r} - \frac{u}{r^2} + \frac{\partial^2 u}{\partial z^2}\right), \tag{4.6}$$

$$\rho_{nf}\left(u\frac{\partial v}{\partial r} + w\frac{\partial v}{\partial z} + \frac{uv}{r}\right) = \mu_{nf}\left(\frac{\partial^2 v}{\partial r^2} + \frac{1}{r}\frac{\partial v}{\partial r} - \frac{v}{r^2} + \frac{\partial^2 v}{\partial z^2}\right), \tag{4.7}$$

$$\rho_{nf}\left(u\frac{\partial w}{\partial r} + w\frac{\partial w}{\partial z}\right) + \frac{\partial p}{\partial z} = \mu_{nf}\left(\frac{\partial^2 w}{\partial r^2} + \frac{1}{r}\frac{\partial w}{\partial r} + \frac{\partial^2 w}{\partial z^2}\right), \tag{4.8}$$

and

$$(\rho c_p)_{nf}\left(u\frac{\partial T}{\partial r} + w\frac{\partial T}{\partial z}\right) = k_{nf}\left(\frac{\partial^2 T}{\partial r^2} + \frac{1}{r}\frac{\partial T}{\partial r} + \frac{\partial^2 T}{\partial z^2}\right) + \mu_{nf}\left[\left(\frac{\partial u}{\partial z}\right)^2 + \left(\frac{\partial v}{\partial z}\right)^2\right], \tag{4.9}$$

Here, μ_{nf} is the dynamic viscosity, ρ_{nf} is the density of nanofluid and k_{nf} is the thermal conductivity nanofluid, which are defined below.

$$\rho_{nf} = (1-\phi)\rho_f + \phi\rho_p\,, \tag{4.10}$$

$$(\rho c_p)_{nf} = (1-\phi)\left(\rho c_p\right)_f + \left(\rho c_p\right)_p, \tag{4.11}$$

$$\frac{k_{nf}}{k_f} = \frac{k_p+2k_f+2\phi(k_f-k_p)}{k_p+2k_f-\phi(k_f-k_p)}, \tag{4.12}$$

and

$$\mu_{nf} = \frac{\mu_f}{(1-\phi)^{2.5}}. \tag{4.13}$$

ϕ is the nanoparticle quantity fraction, $\left(\rho c_p\right)_{nf}$ is the heat capacitance of the nanofluid and k_{nf} is the useful thermal conductivity of the nanofluid. The surface of the rotating disk is kept at a constant temperature T_w and the temperature and pressure of the ambient nanofluid are T_∞ and P_∞.

The corresponding BCs are:

$$u = 0,\ v = \omega r,\ w = 0\,,\ T = T_w\ at\ z = 0, \tag{4.14}$$

$$u \to 0,\ v \to 0\,,\ p \to p_\infty\,,\ T \to T_\infty\ \ at\ z \to \infty\,, \tag{4.15}$$

In which the velocity components u, v, and w are in the direction of increasing r, ϕ, and z, respectively.

Von Karman transformations are defined as below;

$$u = r\omega F(\xi)\,,\quad v = r\omega G(\xi),\ w = \sqrt{\omega\nu_f}H(\xi)\,,\ \ z = \frac{\sqrt{\nu_f}}{\omega}\xi\,,\ p - p_\infty = -p\nu_f\omega P\,,$$

$$\theta = \frac{T-T_\infty}{T_w-T_\infty}, \tag{4.16}$$

where ν is the fluid's kinematic viscosity, ξ denotes a non-dimensional distance along the axis of rotation. F, G, H, and P denotes the non-dimensional functions of ξ. The dimensionless forms of the equation are

$$\left(\frac{d^2F}{d\xi^2}\right) - (1-\phi)^{2.5}\{(1-\phi) + \frac{\phi\rho_p}{\rho_f}\left(F^2 + H\frac{dF}{d\xi} - G^2\right)\} = 0, \tag{4.17}$$

$$\left(\frac{d^2G}{d\xi^2}\right) - (1-\phi)^{2.5}\{(1-\phi) + \frac{\phi\rho_p}{\rho_f}\left(FG + H\frac{dG}{d\xi} + FG\right)\} = 0, \tag{4.18}$$

$$\left(\frac{d^2H}{d\,\xi^2}\right)-\frac{(1-\phi)^{2.5}}{(1-\phi)+\phi\frac{\rho_p}{\rho_f}}\,H\frac{dH}{d\xi}+\frac{(1-\phi)^{2.5}}{(1-\phi)+\phi\frac{\rho_p}{\rho_f}}\left[\left(1-\phi\right)\rho_f+\phi\rho_p\right)\frac{dp}{dz}]=0, \tag{4.19}$$

$$\frac{d^2\theta}{d\xi^2}+PrEc\frac{1}{(1-\phi)^{2.5}}\times[(\left(\frac{dF}{d\xi}\right)^2+\left(\frac{dG}{d\xi}\right)^2]\times\frac{\left[k_p+2k_f-\phi\left(k_f-k_p\right)\right]}{\left[k_p+2k_f+2\,\phi\left(k_f-k_p\right)\right]}-PrH\frac{d\theta}{d\xi}\times$$

$$\frac{\left[k_p+2k_f-\phi\ \left(k_f-k_p\right)\right][(1-\phi)+\phi\frac{(\rho c_p)_p}{(\rho c_p)_f}]}{\left[k_p+2k_f+2\,\phi\left(k_f-k_p\right)\right]}=0, \tag{4.20}$$

With dimensionless boundary conditions are defined below.

$$F\ =\ 0, G\ =\ 1,\ H\ =\ 0\quad \text{when}\quad \xi=0\,, \tag{4.21}$$

$$F\to 0,\ G\to\ 0,\ p\to\ 0\qquad \text{when}\ \xi\to\infty\,, \tag{4.22}$$

and

$$\theta(0)=1,\ \theta(\infty)=\ 0. \tag{4.23}$$

4.3 Entropy Generation

The expression for entropy generation is defined below

$$S_G=\frac{k_{nf}}{(T_\infty)^2}\left(\frac{\partial T}{\partial z}\right)^2+\frac{\mu_{nf}}{T_\infty}[\left(\frac{\partial u}{\partial z}\right)^2+\left(\frac{\partial v}{\partial z}\right)^2]\,,$$

where S_G is Entropy generation, k_{nf} is the thermal conductivity. μ_{nf} is the thickness of the liquid part and. T_∞ is the temperature of ambient temperature. By using similarity transformations in Eqs (4.24) then, we get the following equation:

$$\frac{S_G}{\frac{k_f\Delta T^2\omega}{(T_\infty)^2\upsilon_f}}=\frac{\left[k_p+2k_f+2\phi\left(k_f-k_p\right)\right]}{\left[k_p+2k_f-\phi\left(k_f-k_p\right)\right]}\left(\frac{d\theta}{d\xi}\right)^2+\frac{PrEc}{\Omega}\frac{1}{(1-\phi)^{2.5}}\times[\left(\frac{dF}{d\xi}\right)^2+\left(\frac{dG}{d\xi}\right)^2], \tag{4.25}$$

where

$$\frac{k_f\Delta T^2\omega}{(T_\infty)^2\upsilon_f}\ =\ S_{G_0}\ \text{and}\ \ PrEc\ =Br\,, \tag{4.26}$$

$$\frac{S_G}{S_{G_0}}=\ \frac{\left[k_p+2k_f+2\phi\left(k_f-k_p\right)\right]}{\left[k_p+2k_f-\phi\left(k_f-k_p\right)\right]}.\left(\frac{d\theta}{d\xi}\right)^2+\frac{Br}{\Omega}\frac{1}{(1-\phi)^2}\times[\left(\frac{dF}{d\xi}\right)^2+\left(\frac{dG}{d\xi}\right)^2\,, \tag{4.27}$$

$$N_s = \frac{S_G}{S_{G_0}}, \Omega = \frac{\Delta T}{T_\infty} \text{ and } Ns = N_{SH} + N_{SF}. \quad (4.28)$$

In which N_{SH} represents the entropy generation number due to heat transfer and N_{GF} denotes the entropy generation number due to viscous dissipation.

4.4 Physical parameter

Skin friction coefficient

The quantity C_f is given by,

$$C_f = \frac{\sqrt{\tau_{wr}^2 + \tau_{w\emptyset}^2}}{\rho_f(\omega r)^2} \quad , \quad (4.29)$$

here Ωr are the radial and transversal skin friction coefficients

$$\tau_{wr} = [\mu_{nf}(u_z + w_\emptyset)] \quad at \quad z = 0,$$

$$\tau_{w\emptyset} = \left[\mu_{nf}\left(v_z + \frac{1}{r}w_\emptyset\right)\right] \quad at \quad z = 0\,, \quad (4.30)$$

Putting Eq (4.29) into (4.30), we have,

$$Re^{\frac{1}{2}}C_f = \frac{1}{(1-\phi)^{2.5}}\sqrt{F'(0)^2 + G'(0)^2}\,, \quad (4.31)$$

Nusselt Number

The quantity Nu is given by,

$$Nu = \frac{rq_w}{(T_w - T_\infty)}, \quad (4.32)$$

Where Nu is shear stress at the surface of the disc, and surface temperature flux is denoted by q_w and defined as;

$$q_w = -k_{nf}(T_z) \quad at \quad z = 0 \quad (4.33)$$

Putting Eq. (4.32) into (4.33), we have

$$Re^{-\frac{1}{2}}Nu = -\frac{k_{nf}}{k_f}\theta'(0)\,. \tag{4.34}$$

where $Re = \frac{\omega r^2}{\nu_f}$ is the local Reynolds number.

4.5 Methodology

Eqs. (4.17)-(4.20) with boundary conditions (4.21)-(4.23) are sets of nonlinear ODE that are solved using MATLAB bvp4c tool. The mathematical solution for the converted system is defined as follows:

$x_1 = F\,,\ x_2 = F',\ x_3 = G\,,\ x_4 = G',\ x_5 = H\,, x_6 = \theta, x_7 = \theta'$ as follows:

$$x_1' = x_2, \qquad x_1(0) = 0,$$

$$x_2' = (1-\phi)^{2.5}\left(1-\phi+\phi\frac{\rho_s}{\rho_f}\right)(\,x_2x_5 + x_1^2 - x_3^2)\,, \qquad x_2(0) = s^1,$$

$$x_3' = x_4\,, \qquad x_3(0) = 1,$$

$$x_4' = (1-\phi)^{2.5}\left(1-\phi+\phi\frac{\rho_s}{\rho_f}\right)(x_5x_4 + 2x_1x_3)\,, \qquad x_4(0) = s^3,$$

$$x_5' = -2x_1\,, \qquad x_5(0) = 0,$$

$$x_6' = x_7, \qquad x_6(0) = 1,$$

$$x_7' = \frac{[k_p+2k_f-\phi(k_f-k_p)]}{[k_p+2k_f+2\phi(k_f-k_p)]}\left[(1-\phi)+\phi\,\frac{(\rho c)_p}{(\rho c)_f}\right](Pr)x_5x_7 -$$

$$\frac{1}{(1-\phi)^{2.5}}\frac{[k_p+2k_f-\phi(k_f-k_p)]}{[k_p+2k_f+2\phi(k_f-k_p)]}PrEc(x_2^2+x_4^2), \qquad x_4(0) = s^6,$$

where s^1, s^3 and s^6 are chosen to be $x_1(\infty) = 0, x_3(\infty) = 0\,, x_6(\infty) = 0$. The width of the boundary layer in the given equation is represented by "infinity". The numerical solution for differential equations for the considered fluid model along with boundary conditions is obtained by build-in bvp4c technique using MATLAB. In the typical Newtonian fluid case, our findings are comparable to earlier investigations of Rashidi *et al.* [24].

4.6 Results and Discussion

In this section, the flow of nanofluid over the surface of the rotating disc is examined, and the entropy generation is investigated. The base fluid that we have considered is methanol, and the nanoparticle is Al_2O_3. Effects of various parameters are deliberated through graphs. Figure 4.2 shows the effect of nanoparticle volume fraction ϕ on the radial velocity profile $F(\xi)$. As the value of ϕ increases, the radial velocity $F(\xi)$ increases. Effect of ϕ on the tangential velocity profile $G(\xi)$ is shown in Figure. 4.3. With an increase in ϕ, the momentum boundary layer's thickness increases. Figure. 4.4 illustrates the effect of ϕ on the axial velocity profile $H(\xi)$. $H(\xi)$ and the thickness of the boundary layer both decreases with increasing ϕ. Figure. 4.5 illustrates how the influence of the ϕ on the temperature θ is growing. Consequently, increasing ϕ causes the temperature to rise, and consequently, the thermal boundary layer thickness is enhanced. Figure 4.6 illustrates the impact of variation in Brinkmann number Br on temperature profiles. It is obvious from the figure that increases in Br augments the frictional heating within the fluid, which results in an increase in the temperature profile $\theta(\xi)$. Figure. 4.7 shows that when the value of ϕ is increased, then the skin friction is enhanced. Figure 4.8 displays the effects of Brinkmann number Br on Nusselt number $Re^{-1/2}Nu_x$ plotted versus nanoparticle volume fraction ϕ. It can be observed that an increment in Br leads to significant decreases in the Nusselt number. Moreover, the effects of increasing ϕ on $Re^{-1/2}Nu_x$ are also decreasing.

Figures 4.9 and 4.10 show the impact of nanoparticle volume fraction ϕ and Brinkman number Br on the local entropy generation number Ns plotted against ξ. Figure 4.9 presents the impact of variation in ϕ on Ns. As the value of ϕ increases, the value of Ns decreases slightly near the rotating disk. However, as the distance from the disk increases, the impact of ϕ on Ns are increasing. For a fixed value of ϕ, the entropy generation is maximum at the rotating disk and decreases with an increase in distance and becomes asymptotically zero in the far away region. Figure 4.10 shows that when we increase the value of Brinkman number Br, the fluid friction augments, which leads to a rise in entropy generation Ns .

The influence of nanoparticle volume fraction ϕ and Brinkman number (Br) and Bejan number (Be) are displayed in Figures 4.11 and 4.12. Figure 4.11 shows that heat transfer entropy effects are dominant at the surface of the rotating disk and in its vicinity. In contrast, the fluid

friction entropy effects are dominant away from the plate. Furthermore, it is observed from the figure that heat transfer entropy effects become slightly more dominating as ϕ grows within the boundary layer. Figure 4.12 illustrates that the fluid friction dominates at the surface of the rotating disk and is far away from the rotating disk. Furthermore, it is observed from the figure that entropy due to fluid friction becomes significantly dominant within the boundary layer as the value of ϕ augments.

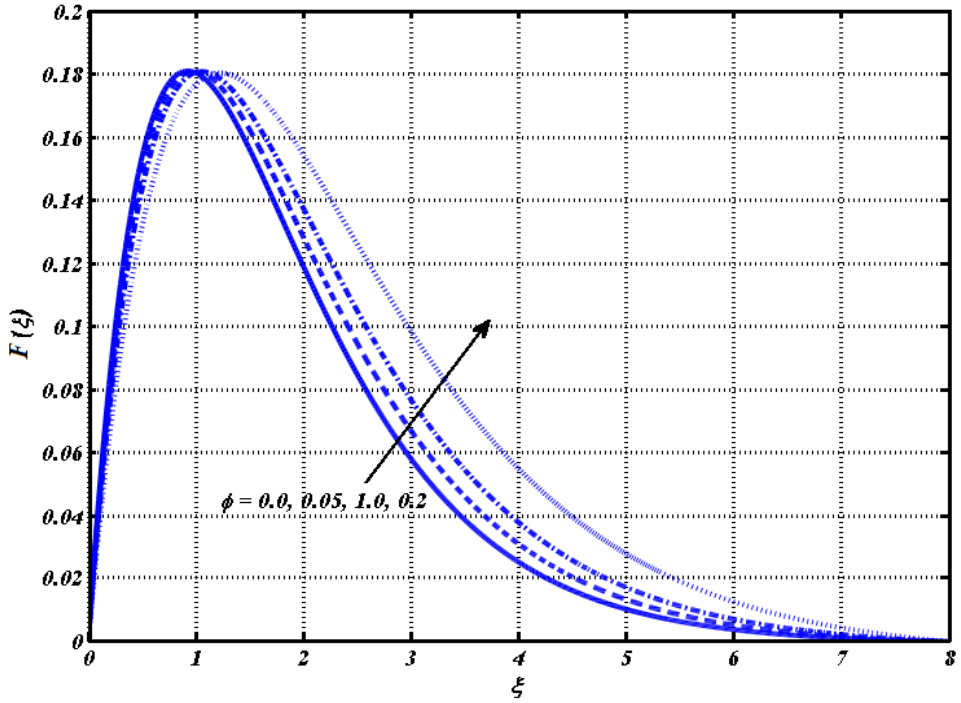

Figure 4.2: Effect of nanoparticle volume fraction ϕ on the radial velocity profile $F(\xi)$.

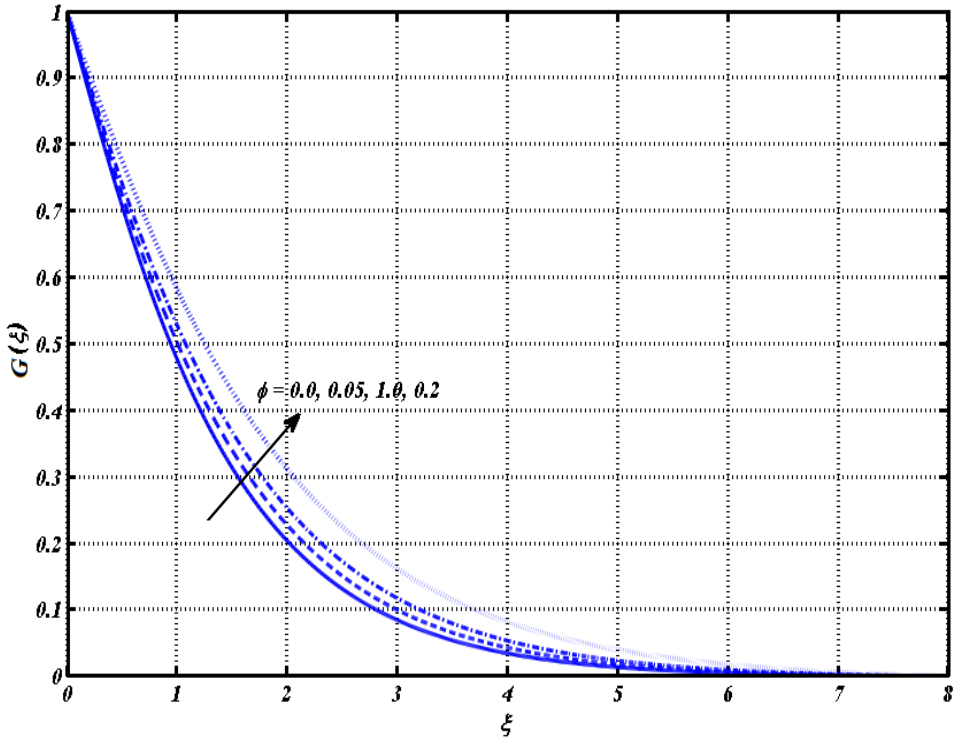

Figure 4.3: Effect of nanoparticle volume fraction ϕ on the tangential velocity profile $G(\xi)$.

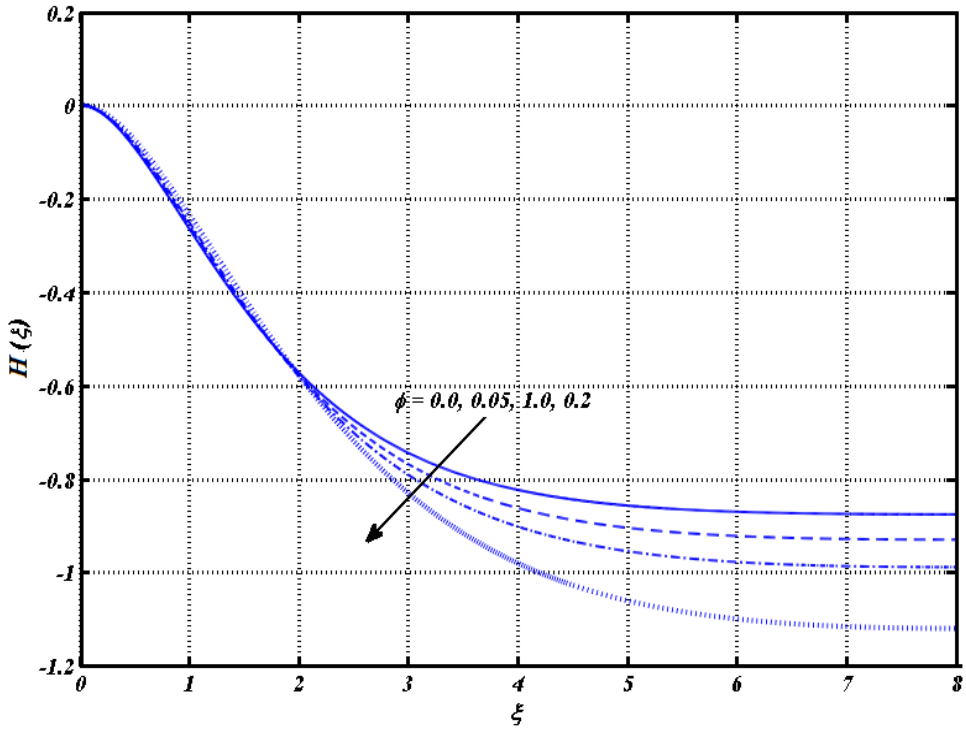

Figure 4.4: Effect of nanoparticle volume fraction ϕ on the axial velocity profile $H(\xi)$.

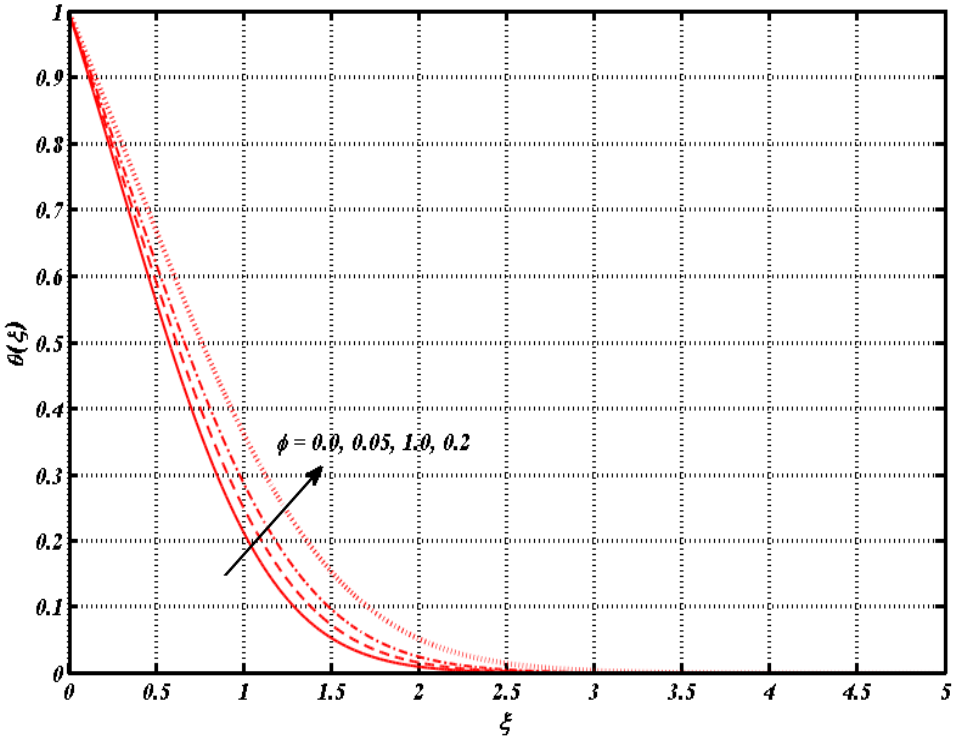

Figure 4.5: Effect of nanoparticle volume fraction ϕ on the temperature profile $\theta(\xi)$.

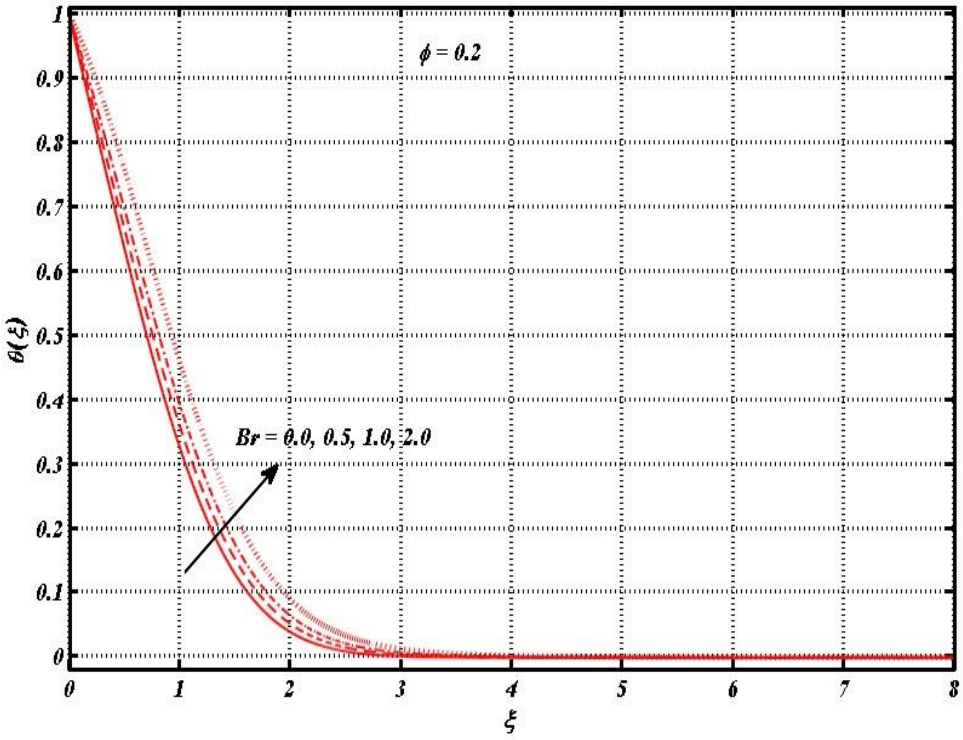

Figure 4.6: Effect of Brinkmann Number *Br* on the temperature profile $\theta(\xi)$.

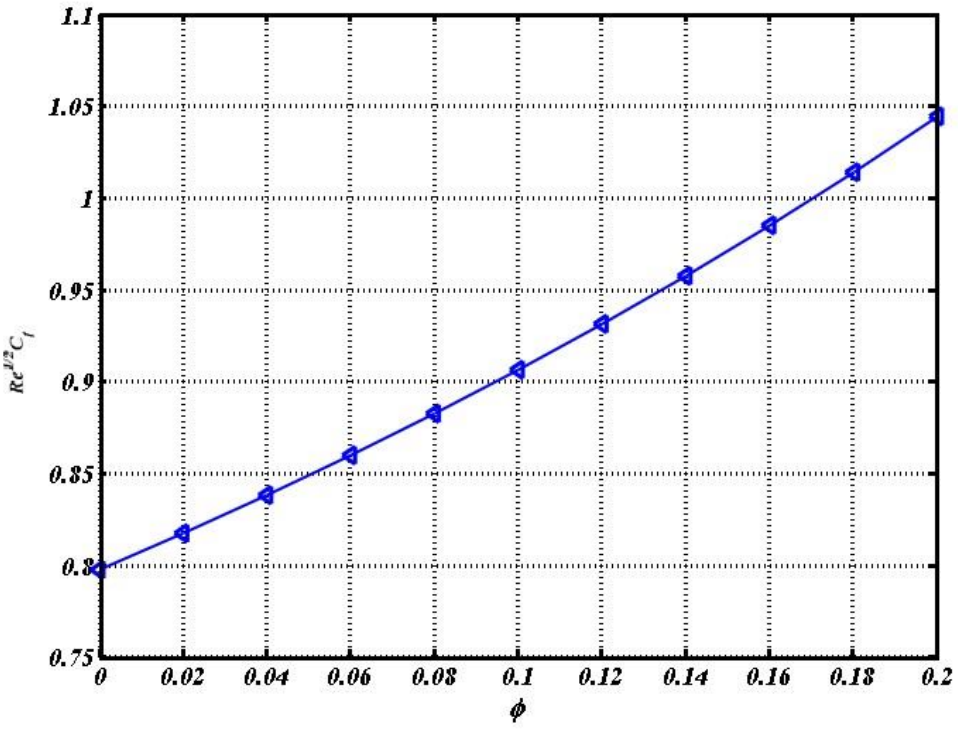

Figure 4.7: Effect of nanoparticle volume friction ϕ on skin friction coefficient $Re^{1/2}C_f$.

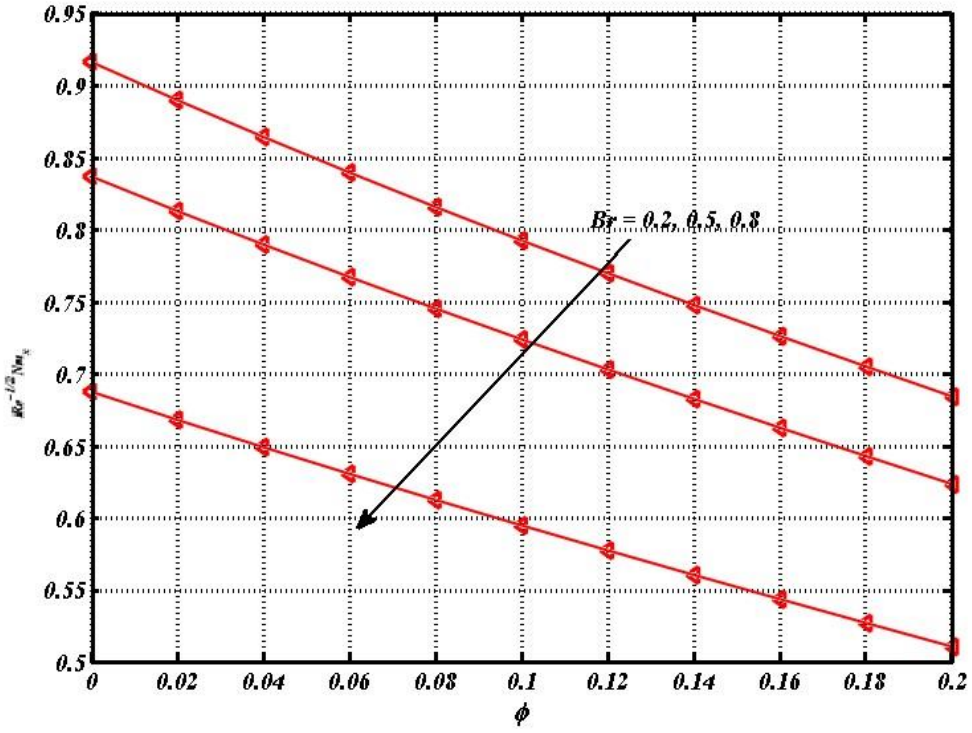

Figure 4.8: Effect of *Br* on Nusselt number $Re^{-1/2}Nu_x$ plotted against ϕ.

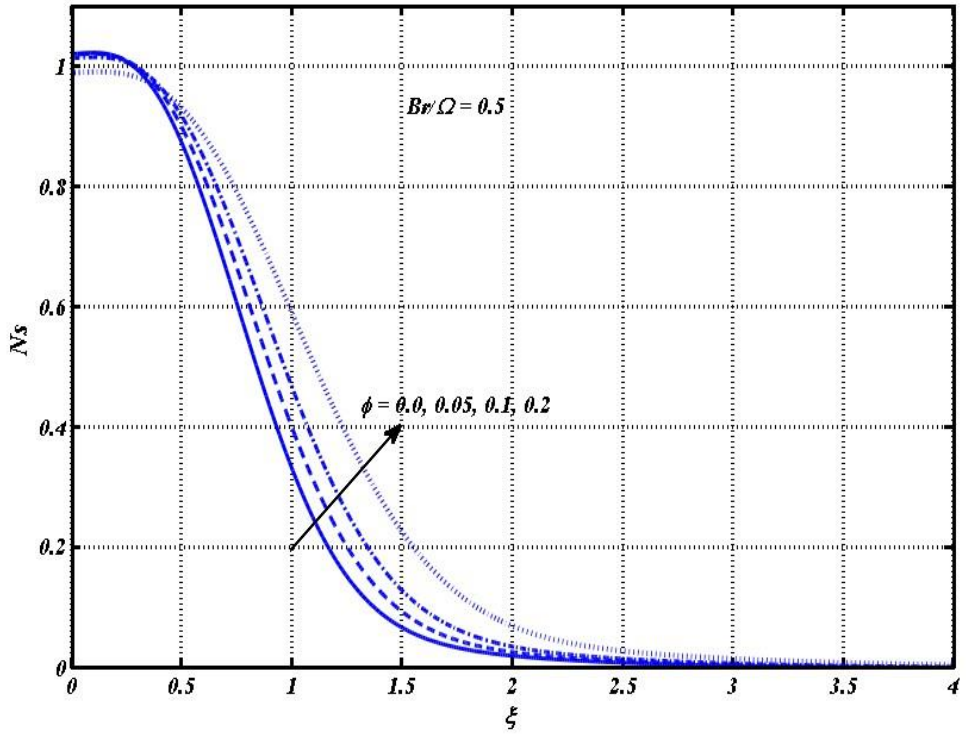

Figure 4.9: Effect of nanoparticle volume fraction ϕ on Entropy generation for rotating disk.

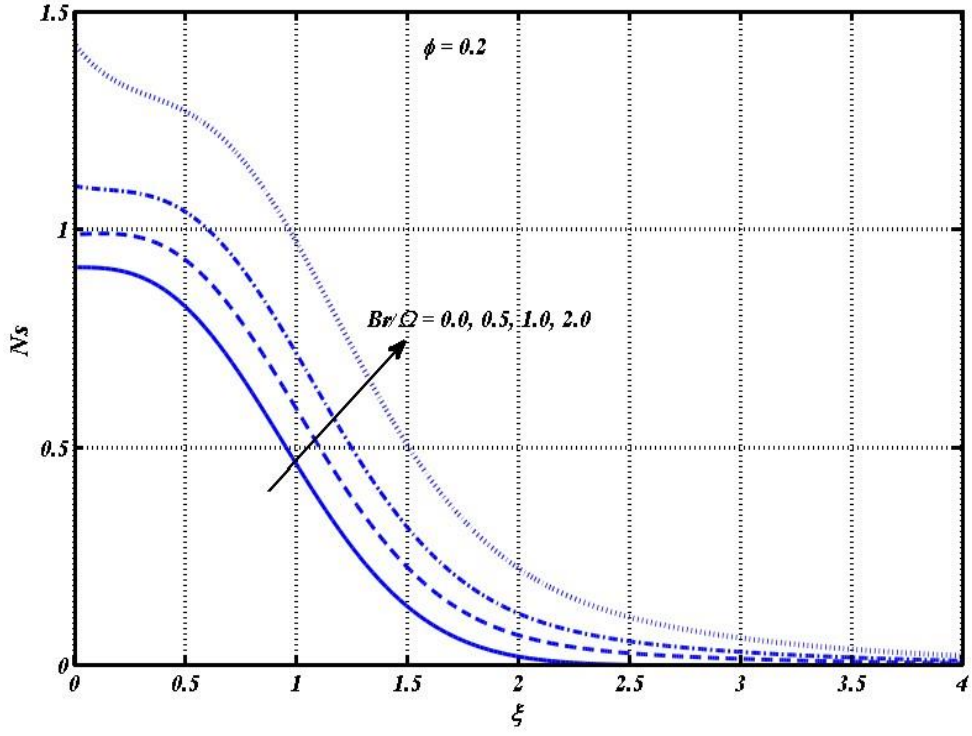

Figure 4.10: Effect of Group parameter (*Br/Ω)* on Entropy generation *Ns.*

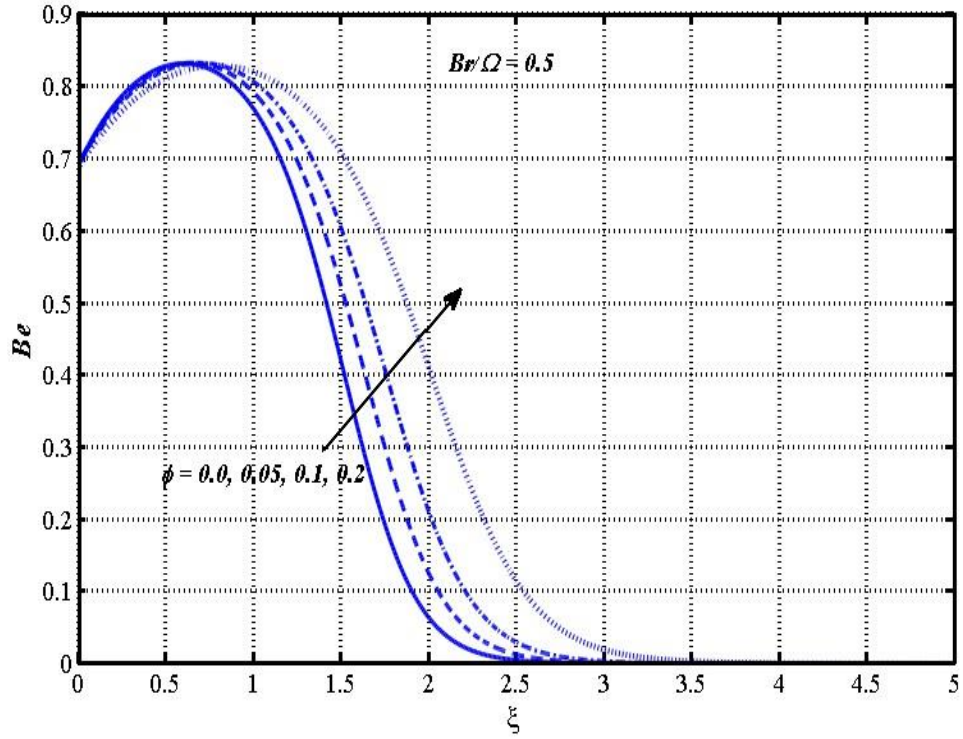

Figure 4.11: Effect of nanoparticle volume fraction ϕ on Bejan number (*Be)*.

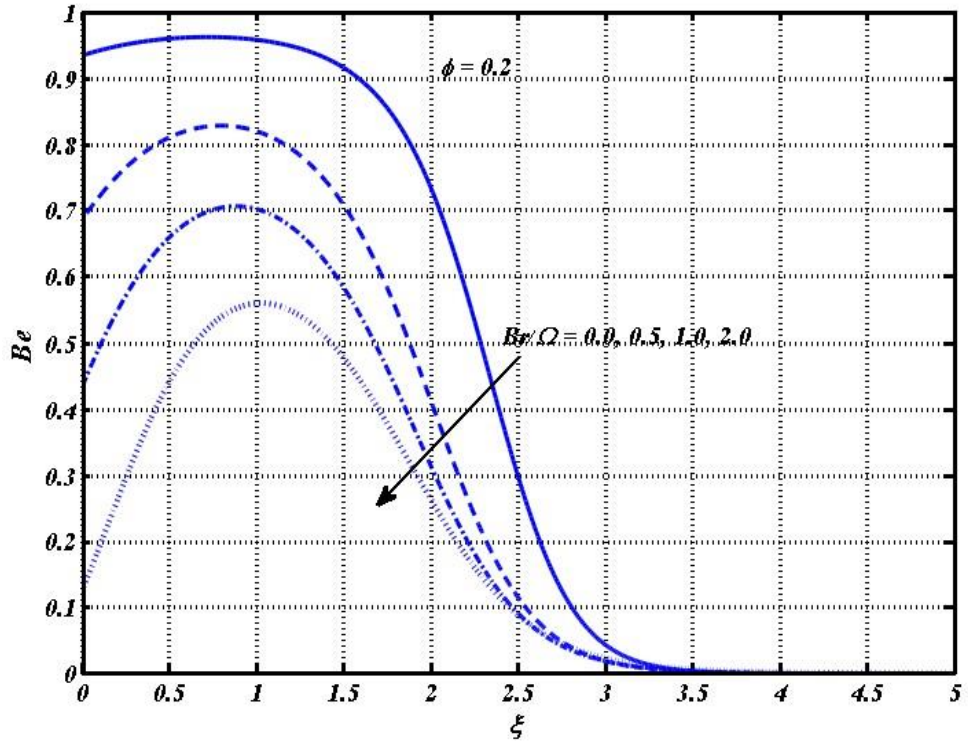

Figure 4.12: Effect of Group parameter *Br/Ω* on Bejan number (*Be)*.

CHAPTER 5

CONCLUSION AND FUTURE WORK

5.1 Overview

This thesis examines the flow and heat transfer phenomena of nanofluid over a rotating disk, and entropy effects are examined. The base fluid is taken to be Methanol, and nanoparticles suspended in it are Al_2O_3. A set of ODEs are derived from nonlinear PDEs by applying the similarity transformations and are solved using the MATLAB routine bvp-4c. The investigation explores the impact of different physical parameters on flow, heat transfer characteristics, and entropy generation. The main findings of the study are as under:

- The radial velocity $F(\xi)$ decreases with an increase in the value of nanoparticle volume concentration (ϕ).
- A decrease in the velocity component $H(\xi)$ is observed as the value of ϕ augments.
- An enhancement in the thermal boundary layer thickness is witnessed as ϕ increases.
- The influence of Brinkmann number Br on temperature profiles $\theta(\xi)$ is increasing.
- There is an increase in skin friction coefficient with an increase in the value of ϕ.
- An increase in the values of nanoparticle volume concentration ϕ and Brinkmann number Br results in a decrease in the Nusselt number $Re^{-\frac{1}{2}}Nu_x$.
- There is a slight decrease in the value of the entropy generation number Ns in the vicinity of the rotating disk as the amount of ϕ increases. However, the effects of increasing the value of ϕ on Ns are increasing as the distance from the disk increases.
- An increase in the value of Brinkman number Br results in augmentation of entropy generation number Ns.

- For the nanoparticle volume concentration, the heat transfer entropy effects are significant at the surface of the rotating disk and in its neighboring region. In contrast, the fluid friction entropy effects dominate away from the plate. Furthermore, the heat transfer entropy effects become slightly more dominating as ϕ grows within the boundary layer.
- In the case of Brinkmann number Br, the fluid friction entropy effects dominate at the rotating disk's surface and far away from the rotating disk. These effects become more prominent within the boundary layer region as the value of Br increases.

5.2. Future work

Building on the findings of this study, future research could explore the flow and heat transfer characteristics of nanofluids over rotating disks under more complex conditions. Investigations could include varying the base fluid and nanoparticle combinations to assess their effects on flow dynamics and entropy generation. Additionally, studying the impact of non-Newtonian fluid behavior and the presence of external magnetic fields could provide deeper insights into the behavior of nanofluids in practical applications. Advanced numerical techniques and machine learning algorithms could be employed to optimize the parameters for enhanced heat transfer and reduced entropy generation.

REFERENCES

[1] S. U. S. Choi, "Enhancing thermal conductivity of fluids with nanoparticles," *Am. Soc. Mech. Eng. Fluids Eng. Div. FED*, vol. 231, no. January 1995, pp. 99–105, 1995.

[2] S. Senthilraja, M. Karthikeyan, and R. Gangadevi, "Nanofluid applications in future automobiles: Comprehensive review of existing data," *Nano-Micro Lett.*, vol. 2, no. 4, pp. 306–310, 2010, doi: 10.3786/nml.v2i4.p306-310.

[3] J. Patel, A. Soni, D. P. Barai, and B. A. Bhanvase, "A minireview on nanofluids for automotive applications: Current status and future perspectives," *Appl. Therm. Eng.*, vol. 219, no. PA, p. 119428, 2023, doi: 10.1016/j.applthermaleng.2022.119428.

[4] B. Ali, F. Z. Duraihem, S. Jubair, H. Alqahtani, and B. Yagoob, "Analysis of interparticle spacing and nanoparticle radius on the radiative alumina based nanofluid flow subject to irregular heat source/sink over a spinning disk," *Mater. Today Commun.*, vol. 36, no. June, p. 106729, 2023, doi: 10.1016/j.mtcomm.2023.106729.

[5] S. Ahmad *et al.*, "Thermal and solutal energy transport analysis in entropy generation of hybrid nanofluid flow over a vertically rotating cylinder," *Front. Phys.*, vol. 10, no. September, pp. 1–11, 2022, doi: 10.3389/fphy.2022.988407.

[6] H. Yasmin, S. O. Giwa, S. Noor, and M. Sharifpur, "Thermal Conductivity Enhancement of Metal Oxide Nanofluids: A Critical Review," *Nanomaterials*, vol. 13, no. 3, 2023, doi: 10.3390/nano13030597.

[7] G. F. Smaisim *et al.*, "Nanofluids: properties and applications," *J. Sol-Gel Sci. Technol.*, vol. 104, no. 1, pp. 1–35, 2022, doi: 10.1007/s10971-022-05859-0.

[8] S. Afzal, M. Qayyum, and G. Chambashi, "Heat and mass transfer with entropy optimization in hybrid nanofluid using heat source and velocity slip: a Hamilton–Crosser approach," *Sci. Rep.*, vol. 13, no. 1, pp. 1–21, 2023, doi: 10.1038/s41598-023-39176-5.

[9] O. Mahian, A. Kianifar, S. A. Kalogirou, I. Pop, and S. Wongwises, "A review of the applications of nanofluids in solar energy," *Int. J. Heat Mass Transf.*, vol. 57, no. 2, pp. 582–594, 2013, doi: 10.1016/j.ijheatmasstransfer.2012.10.037.

[10] Z. Mahmood, S. M. Eldin, K. Rafique, and U. Khan, "Numerical analysis of MHD tri-hybrid nanofluid over a nonlinear stretching/shrinking sheet with heat generation/absorption and slip conditions," *Alexandria Eng. J.*, vol. 76, pp. 799–819,

2023, doi: 10.1016/j.aej.2023.06.081.

[11] K. Rafique *et al.*, “Investigation of thermal stratification with velocity slip and variable viscosity on MHD flow of Al2O3−Cu−TiO2/H2O nanofluid over disk,” *Case Stud. Therm. Eng.*, vol. 49, no. June, p. 103292, 2023, doi: 10.1016/j.csite.2023.103292.

[12] K. Rafique, Z. Mahmood, U. Khan, S. M. Eldin, and A. M. Alzubaidi, “Mathematical analysis of radius and length of CNTs on flow of nanofluid over surface with variable viscosity and joule heating,” *Heliyon*, vol. 9, no. 7, p. e17673, 2023, doi: 10.1016/j.heliyon.2023.e17673.

[13] M. A. Basit *et al.*, “Comprehensive investigations of (Au-Ag/Blood and Cu-Fe3O4/Blood) hybrid nanofluid over two rotating disks: Numerical and computational approach,” *Alexandria Eng. J.*, vol. 72, pp. 19–36, 2023, doi: 10.1016/j.aej.2023.03.077.

[14] S. A. M. Mehryan, M. Izadi, A. J. Chamkha, and M. A. Sheremet, “Natural convection and entropy generation of a ferrofluid in a square enclosure under the effect of a horizontal periodic magnetic field,” *J. Mol. Liq.*, vol. 263, pp. 510–525, 2018, doi: 10.1016/j.molliq.2018.04.119.

[15] G. Huminic and A. Huminic, “Entropy generation of nanofluid and hybrid nanofluid flow in thermal systems: A review,” *J. Mol. Liq.*, vol. 302, 2020, doi: 10.1016/j.molliq.2020.112533.

[16] M. I. Khan and F. Alzahrani, “Nonlinear dissipative slip flow of Jeffrey nanomaterial towards a curved surface with entropy generation and activation energy,” *Math. Comput. Simul.*, vol. 185, pp. 47–61, 2021, doi: 10.1016/j.matcom.2020.12.004.

[17] R. Akhter, M. Mokaddes Ali, and M. A. Alim, “Entropy generation due to hydromagnetic buoyancy-driven hybrid-nanofluid flow in partially heated porous cavity containing heat conductive obstacle,” *Alexandria Eng. J.*, vol. 62, pp. 17–45, 2023, doi: 10.1016/j.aej.2022.07.005.

[18] S. A. Khan, T. Hayat, and A. Alsaedi, “Entropy generation in chemically reactive flow of Reiner-Rivlin liquid conveying tiny particles considering thermal radiation,” *Alexandria Eng. J.*, vol. 66, pp. 257–268, 2023, doi: 10.1016/j.aej.2022.11.027.

[19] K. Rafique, Z. Mahmood, H. Alqahtani, and S. M. Eldin, “Various nanoparticle shapes and quadratic velocity impacts on entropy generation and MHD flow over a stretching sheet with joule heating,” *Alexandria Eng. J.*, vol. 71, pp. 147–159, 2023, doi: 10.1016/j.aej.2023.03.021.

[20] B. K. Sharma, A. Kumar, R. Gandhi, M. M. Bhatti, and N. K. Mishra, “Entropy Generation and Thermal Radiation Analysis of EMHD Jeffrey Nanofluid Flow:

Applications in Solar Energy," *Nanomaterials*, vol. 13, no. 3, pp. 1–23, 2023, doi: 10.3390/nano13030544.

[21] W. Ibrahim and D. Gamachu, "Entropy generation in radiative magneto-hydrodynamic mixed convective flow of viscoelastic hybrid nanofluid over a spinning disk," *Heliyon*, vol. 8, no. 12, p. e11854, 2022, doi: 10.1016/j.heliyon.2022.e11854.

[22] O. Mahian *et al.*, "A review of entropy generation in nanofluid flow," *Int. J. Heat Mass Transf.*, vol. 65, pp. 514–532, 2013, doi: 10.1016/j.ijheatmasstransfer.2013.06.010.

[23] R. Kumar, G. S. Seth, and A. Bhattacharyya, "Entropy generation of von Karman's radiative flow with Al2O3 and Cu nanoparticles between two coaxial rotating disks: A finite-element analysis," *Eur. Phys. J. Plus*, vol. 134, no. 12, 2019, doi: 10.1140/epjp/i2019-13086-0.

[24] M. M. Rashidi, S. Mahmud, N. Freidoonimehr, and B. Rostami, "Analysis of entropy generation in an MHD flow over a rotating porous disk with variable physical properties," *Int. J. Exergy*, vol. 16, no. 4, pp. 481–503, 2015, doi: 10.1504/IJEX.2015.069110.

[25] N. A. Khan, N. A. Khan, S. Ullah, and F. Naz, "Swirling flow of couple stress fluid due to a rotating disk," *Nonlinear Eng.*, vol. 8, no. 1, pp. 261–269, 2019, doi: 10.1515/nleng-2017-0062.

[26] O. A. Bég, M. N. Kabir, M. J. Uddin, A. Izani Md Ismail, and Y. M. Alginahi, "Numerical investigation of Von Karman swirling bioconvective nanofluid transport from a rotating disk in a porous medium with Stefan blowing and anisotropic slip effects," *Proc. Inst. Mech. Eng. Part C J. Mech. Eng. Sci.*, vol. 235, no. 19, pp. 3933–3951, 2021, doi: 10.1177/0954406220973061.

[27] R. Balaji, J. Prakash, D. Tripathi, and O. Anwar Bég, "Heat transfer and hydromagnetic electroosmotic Von Kármán swirling flow from a rotating porous disc to a permeable medium with viscous heating and Joule dissipation," *Heat Transf.*, vol. 52, no. 5, pp. 3489–3515, 2023, doi: 10.1002/htj.22837.

[28] J. Visuvasam and H. Alotaibi, "Analysis of Von Kármán Swirling Flows Due to a Porous Rotating Disk Electrode," *Micromachines*, vol. 14, no. 3, pp. 1–11, 2023, doi: 10.3390/mi14030582.

[29] P. Rana and G. Gupta, "Sensitivity computation of Von Kármán's swirling flow of nanoliquid under nonlinear Boussinesq approximation over a rotating disk with Stefan blowing and multiple slip effects," *Waves in Random and Complex Media*, 2022, doi: 10.1080/17455030.2022.2112633.

[30] J. C. Umavathi, O. A. Bég, T. A. Bég, and A. Kadir, “Swirling bioconvective nanofluid flow from a spinning stretchable disk in a permeable medium,” *Int. J. Model. Simul.*, vol. 43, no. 5, pp. 764–796, 2023, doi: 10.1080/02286203.2022.2122928.

[31] M. Hussain, M. Rasool, and A. Mehmood, “Radiative flow of viscous nano-fluid over permeable stretched swirling disk with generalized slip,” *Sci. Rep.*, vol. 12, no. 1, pp. 1–19, 2022, doi: 10.1038/s41598-022-15159-w.

[32] T. Hayat, M. Rashid, M. Imtiaz, and A. Alsaedi, “Magnetohydrodynamic (MHD) flow of Cu-water nanofluid due to a rotating disk with partial slip,” *AIP Adv.*, vol. 5, no. 6, 2015, doi: 10.1063/1.4923380.

[33] S. Jain and S. Bohra, “Radiation effects in flow through porous medium over a rotating disk with variable fluid properties,” *Adv. Math. Phys.*, vol. 2016, 2016, doi: 10.1155/2016/9671513.

[34] X. H. Zhang, E. A. Algehyne, M. G. Alshehri, M. Bilal, M. A. Khan, and T. Muhammad, “The parametric study of hybrid nanofluid flow with heat transition characteristics over a fluctuating spinning disk,” *PLoS One*, vol. 16, no. 8 August, pp. 1–17, 2021, doi: 10.1371/journal.pone.0254457.

[35] H. A. Attia, “Steady flow over a rotating disk in porous medium with heat transfer,” *Nonlinear Anal. Model. Control*, vol. 14, no. 1, pp. 21–26, 2009, doi: 10.15388/na.2009.14.1.14527.